RTM for Waste Repositories

Olivier Bildstein, Francis Claret, Pierre Frugier

Reviews in Mineralogy & Geochemistry
Vol. 85 pp. 419-457, 2019

RTM for Waste Repositories

Olivier Bildstein

Commissariat à l'Énergie Atomique et aux Énergies Alternatives (CEA)
Direction de l'Energie Nucléaire (DEN)
Cadarache
DTN, SMTA, LMTE
F-13108 Saint-Paul-Lez-Durance
France

olivier.bildstein@cea.fr

Francis Claret

Bureau de Recherches Géologiques et Minières
3 Avenue Guillemin
F-45060, Orléans Cedex 2
France

francis.claret@brgm.fr

Pierre Frugier

Commissariat à l'Énergie Atomique et aux Énergies Alternatives (CEA)
Direction de l'Energie Nucléaire (DEN)
Marcoule
DTCD, SECM, LCLT
F-30207 Bagnols-sur-Cèze Cedex
France

pierre.frugier@cea.fr

INTRODUCTION

A need for numerical simulations

Power generation plays an important role in global warming (Audoly et al. 2018) and although the use of nuclear power in the energetic mix can be seen as sustainable (Brook et al. 2014; Knapp and Pevec 2018), nuclear energy is debated in many countries (Meserve 2004; Cici et al. 2012). Over 50 years of nuclear energy and the use of radioactive material in nuclear research and in industrial, medical and other applications have left a legacy of different kinds of nuclear waste awaiting final disposal worldwide. To ensure very long-term isolation to protect the environment and ensure the safety of the future generations (Linsley and Fattah 1994; Hummel and Schneider 2005), geological disposal facilities ('repositories') are considered to be the most suitable solution. When the activity in waste is relatively low and half-lives are less than about 30 a, i.e. for intermediate- and low-level waste, near-surface disposal is often considered to be adequate. For waste with a higher activity and/or longer life, i.e. for high-level long-lived waste (HLLW), the concept of geological disposal of radioactive waste emerged in the late 1950s (Hess 1957; De Marsily et al. 1977; Apted and Ahn 2010; Chapman and Hooper 2012). Since then, many international research and development programs have been launched to study deep argillaceous formations, granitic rocks and salt formations as potential host rocks for radioactive waste disposal (Landais and Aranyossy 2011)(Fig. 1).

1529-6466/19/0085-0014$05.00 (print)
1943-2666/19/0085-0014$05.00 (online)
http://dx.doi.org/10.2138/rmg.2019.85.14

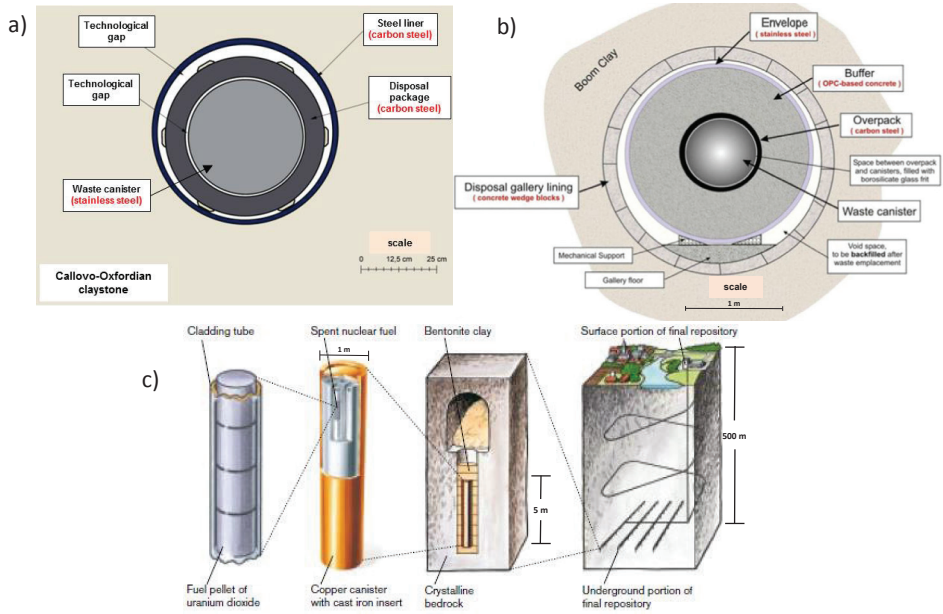

Figure 1. Schematic view of repository concepts/disposal cells in clay host rock **a)** without concrete (modified from Andra 2005), **b)** with concrete Supercontainer (modified from Ondraf/Niras 2009), and **c)** in granitic host-rock (modified from SKB 2006).

Based on their outcomes, there is a broad technical consensus that geologic disposal will meet the safety requirement to minimize safety and environmental impacts, now and far into the future (Grambow and Bretesché 2014), meaning a hundred thousand to million years into the future. Demonstrating safety over time comparable to geological timescales relies on a rigorous, complex and iterative scientific approach referred to as "long-term behavior science" that is based upon three pillars: experiments, modeling, and natural/archaeological analogs (Poinssot and Gin 2012; Dillmann et al. 2014; Alexander et al. 2015; Martin et al. 2016). Today, numerical models are ubiquitous tools that can be used either for long-term predictive evaluation of solute transport or design optimization of nuclear waste geologic repositories (Tsang et al. 1994; Johnson et al. 2017). They are also used to make predictive multi-physical assessments within a timeframe and space scale larger than experiments can cover (Bredehoeft 2003; Bildstein and Claret 2015). These numerical simulations require integrating, in a consistent framework, an increasing amount of scientific knowledge (Geckeis and Rabung 2008) acquired for each of the individual components of such repositories. This implies considering couplings of different non-linear processes, applied to a wide range of materials with contrasting properties as a function of time and space in ever-larger systems. Reactive transport modeling (Yeh and Tripathi 1989) has established itself as a powerful, versatile and essential tool for tackling the complexity of the multi-space and temporal-scale issues engineers and scientists face. This includes describing the evolution of the components constituting the so-called "multiple-barrier system" between the waste matrix and the biosphere (Apted and Ahn 2010; Chapman and Hooper 2012). Predicting how (i) the waste matrices (e.g., glass, bitumen, cement), (ii) waste overpacks (e.g., metal canisters, concrete), (iii) engineered barriers such as bentonite (Sellin and Leupin 2013), (iv) and natural geological barriers will evolve with time in response to physical and chemical perturbations is of prime

importance for performance and safety evaluations of the repository concepts. This chapter summarizes recent improvements and discusses future challenges in the application of reactive transport to deep geological nuclear waste disposal focusing on disposal in clay formations.

A need to consider coupled processes

The long-term safety of geological disposal is based on the multi-barrier concept consisting of a combination of natural (host rocks) and engineered (waste form, package, backfill and seal materials) barriers that will have mutual interactions during the lifetime of the repository. Predicting the effects of these interactions entails understanding, evaluating and prioritizing the pertinent thermal, hydraulic, mechanical, chemical and radiological (THMCR) processes (Fig. 2).

Thermal effects arise principally from heat generated by waste that is both dissipated in the over-packs and the geological medium, and evacuated by air ventilation (Benet et al. 2014a).The hydraulic stage and gas-related effects are a combination of repository resaturation and of gas generation. (e.g., H_2 production by anaerobic corrosion of metals or through water radiolysis). The hydraulic transient is also impacted upon by the ventilation systems used during the operation period to ensure adequate gallery aeration for the workers and for the infrastructure. It will create heat and vapor exchanges with walls and storage packages, pressure variations and evaporation, and sometimes vapor condensation (Benet et al. 2014b). Mechanical effects can be induced during construction and excavation of underground drifts that will cause both tunnel convergence (Lisjak et al. 2015) and damage to the rock in the vicinity of the opening, with the formation of an associated excavated disturbed zone (EDZ) (Armand et al. 2014). There are also numerous chemical effects as foreign materials like borosilicate glasses (Poinssot et al. 2010; Gin et al. 2015), metallic canisters (King and Shoesmith 2010), and concrete (Alonso et al. 2010) that are introduced into the repository will induce chemical gradients across the repository components (Nagra 2002; Andra 2005, 2009). Because of these chemical gradients, perturbations such as pH and redox changes may alter the performance of the barriers over time

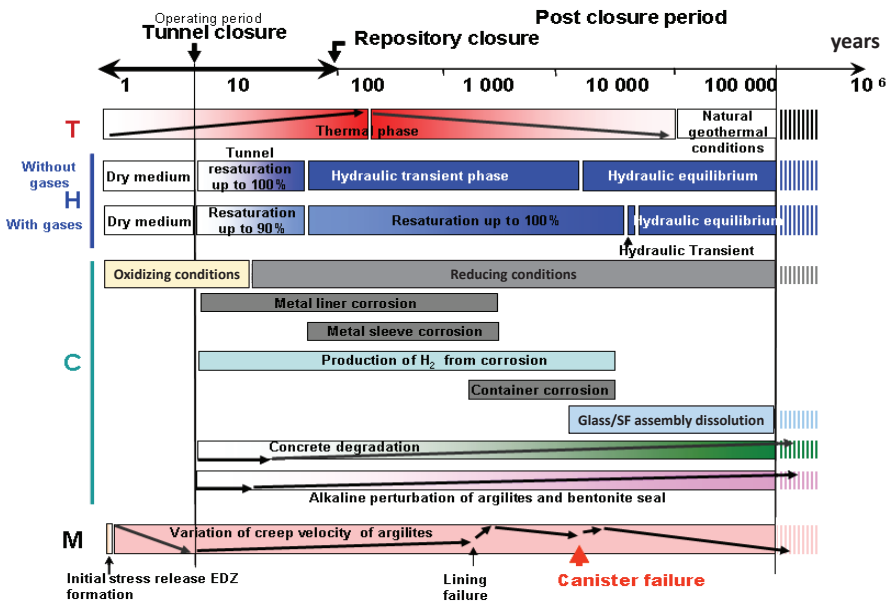

Figure 2. Phenomenological evolution of the repository in high-level long-lived waste (HLLW) and intermediate-level long-lived waste (ILLW) quarters showing timescale of THMC processes (modified from Andra 2005).

(Bildstein and Claret 2015). Last but not least, radiological effects also exist in association with the radiological inventory of waste independently from the technological solution, retreatment or direct disposal of irradiated fuels (Odorowski et al. 2017) or after reprocessing (Gong et al. 1999; Berner et al. 2013). Moreover, an additional challenge arises because all of the THMC phenomena described above are coupled. The coupling of physical and chemical phenomena can be either weak or strong and may vary in time and space scales. As an illustration, excavation induces a mechanical rock effect producing an EDZ. The change in rock microstructure in the EDZ compared to pristine rock might impact radionuclide (RN) transport parameters if this damage zone acts as a preferential pathway for fluid flow and RN transport. However, issues are more complicated as the EDZ can heal and seal itself depending on hydraulic conditions (Thatcher et al. 2016). Another example of a coupled process is the evolution of redox conditions, a key parameter for RN solubility (Duro et al. 2014) which can be modified in connection with hydraulic and mechanical process. The oxidation event that will also occur in the repository near field (Matray et al. 2007; Craen et al. 2008; Vinsot et al. 2013; De Windt et al. 2014; Vinsot et al. 2014) as result of excavation and ventilation will change redox conditions. These conditions could also been modified if radiological effects are considered. The radiolysis effects of water under alpha irradiation simultaneously producing oxidizing species (e.g., hydrogen peroxide), and reducing species like hydrogen might play a role when competing with redox active species from the ambient environment (Odorowski et al. 2017). Many other examples of features and processes and their relevance in performance assessment and safety cases are given by (Bernier et al. 2017), including microbiological effects. These combined processes may be detrimental or favorable to the overall performance of a repository system over time. Since the combinations will occur on time-scales that are not accessible to experimentation, we must develop modeling approaches that can help to predict how barriers will evolve in time and space (Claret et al. 2018b). Reactive transport modeling is probably one of the most efficient techniques used to account for and quantify the complexity of coupling processes over a long period of time. Many codes exist (see Steefel et al. 2015b for a recent review) and to our knowledge, none of them are able to integrate all coupled THMCR effects. However, since the 34th volume of *Reviews in Mineralogy* (dedicated to reactive transport in porous media) was published about 20 years ago, numerical codes have continuously improved and are capable of representing more and more complex situations. Active topics of research dealing with RTM include the development of pore scale and hybrid, or multiple continua, models to capture the scale dependence of coupled reactive transport processes (Steefel et al. 2005). In this chapter, most of the reviewed studies that are described are based on continuum models (Lichtner 1996), although other kinds of approaches will be addressed at the end.

REACTIVE TRANSPORT MODELING

Governing equations

The reactive transport constitutive equations rely on the description of the porous medium of interest (e.g., one of the component of the multi-barrier system) at the continuum scale, with respect to its macroscopically measurable properties such as permeability, dispersivity and diffusability (Steefel et al. 2014, 2015b). In this framework, a generic equation for advective/dispersive transport in the liquid phase coupled to bio-geochemical reactions can be written:

$$\frac{\partial\left(\phi S_{\mathrm{L}}\Psi_i\right)}{\partial t}=\nabla\left(\phi S_{\mathrm{L}}D_i^{*}\nabla\Psi_i\right)-\nabla\left(q\Psi_i\right)-\sum_{r=1}^{Nr}\nu_{ir}R_r-\sum_{m=1}^{Nm}\nu_{im}R_m-\sum_{s=1}^{Ns}\nu_{is}R_s-\sum_{l=1}^{Nl}\nu_{il}R_l \qquad (1)$$

$$\Psi_i=C_i+\sum_{j=1}^{N_x}\nu_{ji}\cdot C_j \qquad (2)$$

where ϕ is the porosity ($m^3_{void} \cdot m^{-3}_{medium}$), S_L is the liquid saturation (unitless), $\emptyset_i$ ($mol \cdot m^{-3}_{water}$) is the total concentration term that integrates the distribution between primary species (with concentration C_i) and secondary species ($\sum_{j=1}^{N_s} \nu_{ji} \cdot C_j$), D_i^* is the diffusion coefficient for species i in the porous media ($m^2 \cdot s^{-1}$), q is the volumetric (or Darcy flux) of water ($m^3_{water} \cdot m^{-2}_{medium} \cdot s^{-1}$), and R_r, R_m, R_s, and R_l are the aqueous phase, mineral, surface, and gas reactions ($mol \cdot m^3_{medium} \cdot s^{-1}$) respectively. ν_{ji} is the number of moles of component i in one mole of secondary species j. ν_{ik} with $k = r$, m or l is the number of moles of component i in one mole of phase k.

These equations can be expanded to consider (i) transport in phases other than the liquid (e.g., gases), (ii) a dispersion term, or (iii) the Nernst–Planck Equation, instead of Fick's Equation, to model diffusional transport. A comprehensive description of these equations can be found in Steefel et al. (2015b). Recently, the significance of the parameters in Equations (1) and (2), their relationship in case of mutual dependence (e.g., diffusion and saturation permeability and saturation) and the way they can be approximated using different empirical or based on theory laws have been reviewed (Claret et al. 2018b). Therefore, it will not be detailed again here. Equation (1) also highlights the fact that a porosity has to be defined for the considered materials. However, some of them (e.g., steel and other metals, glass) are not porous materials, and, unfortunately, reactive transport models are, by definition and according to Equation (1), not suited to include non-porous media (Bildstein et al. 2007; Claret et al. 2018b). To unravel this problem, the volume clearance that exists at the interface between the canister or the glass and the surrounding material, also known as the "technological gap", is often included in the numerical cells that represent these materials.

The critical need for thermodynamic databases

Inherently, to model reactivity and couple it with transport, geochemical databases are needed. To illustrate this point, let us consider the transport of contaminants in a repository and its relationship with geochemistry. Speciation of the considered element will be a key parameter controlling the species distribution among the different phases and their solubility limits. While the solute species can diffuse with the porewater through the barriers, their precipitation represents an appreciable retardation mechanism (Wanner 2007). Speciation also controls sorption processes that can induce retardation mechanism for transport (Grenthe 1991; Grambow 2008). Nonetheless, it is not only a question of speciation. Transport is also governed by porosity change, and this is why thermodynamic databases should also account for minerals that constitute the barriers and secondary minerals that are able to precipitate when different barriers are in contact. In the field of nuclear energy, database comprehensiveness and consistency are key issues that have been initiated by Nuclear Energy Agencies and later prioritized at the national level (see Ragoussi and Costa 2019 for a review). In addition, the pivotal importance of databases for RTM calculation has recently been the focus of a special issue of *Applied Geochemistry* (Kulik et al. 2015). Within the framework of national radioactive waste disposal projects, database development has focused on consistent data for actinides, lanthanides, and chemotoxics, among other potential contaminants. When modeling disposal conditions, there is also a need to describe the evolution of the materials constituting the barriers. This research effort combines new thermodynamic data acquisition, especially for clay minerals (Gailhanou et al. 2007, 2009, 2012, 2013, 2017; Blanc et al. 2015a) and cement phases (Roosz et al. 2018), critical data selection for repository materials such as cement phases (Blanc et al. 2010; Walker et al. 2016; Lothenbach et al. 2019) and how to evaluate their capacity to describe interactions between materials (Blanc et al. 2015a). In addition, kinetic databases with kinetic rate parameters are being built (Marty et al. 2015a), as well as a sorption database (Brendler et al. 2003). An important constraint for kinetic rate parameters is consistency with the associated thermodynamic database for stoichiometry and solubility values, so that we can calculate how rates depend on saturation states.

Modeling materials and reactive interfaces

Studies on deep geological storage show that most of the physical and chemical reactivity will be concentrated close to the interface between the different materials. A first challenge therefore consists of predicting the extent of the alteration and the distance at which the perturbations will progress into the barriers and, in case of failure, into the waste matrices. Another challenge is to predict the evolution of the material properties in these barriers resulting from their alteration, and to assess the impact on the overall performance and safety of the system.

A non-exhaustive list of interfaces is given in Table 1 with a description of their occurrence in different disposal concepts including clay formations (e.g., in Belgium, France, Spain, and Switzerland) and crystalline host rocks (note that bentonite is used as a barrier between the containers and granite in this case, e.g., in Canada, Spain, and Switzerland). Another degree of complexity is added in HLLW repository concepts from Sweden and Finland where the use of copper containers is envisaged, as well as in France where a bentonitic cement may be emplaced at the extrados of the steel liner to avoid early corrosion in acidic conditions.

Concerning waste matrices, only the specific behavior of vitrified waste (glass) will be detailed in this chapter. For the alteration of spent fuel (SF), the authors refer the reader to the recent review of these aspects by (Ewing 2015). Waste matrices for ILLW *per se* are not detailed in this chapter, but most of the conclusions will be applicable to cementitious and metallic waste types. For bituminous and organic waste, the authors refer the reader to the modeling work of Sercombe et al. (2006), von Schenck and Källström (2014), and De Windt et al. (2015).

The direct interaction of materials with groundwater is not treated specifically in this chapter, even though the authors acknowledge that many interesting studies related to waste disposal in fractured hard rocks, where this issue is particularly relevant, have been conducted. In the disposal concepts that rely upon a chemical buffer of high pH (mainly ILLW), the issue of the interaction of groundwater with cement/concrete has been addressed (see (Wilson et al. 2018) for a recent review). RTM studies of cement-groundwater interactions have been reported with results concerning pH evolution, and chemical and mechanical degradation of concrete barriers (Höglund 2001, 2013; Bamforth et al. 2012; Cronstrand 2014; Wilson et al. 2018). In HLW disposal concepts, the bentonite buffer surrounding waste packages will evolve with time due to progressive reaction with saturating ambient groundwater, including ion exchange, dissolution-precipitation of accessory (gypsum, halite quartz, calcite) and clay minerals potentially affecting properties such as the hydraulic conductivity and the swelling pressure. RTM studies regarding these aspects have evolved from simple exchange models to more complex 1- and 2-D problem setup, including the effect of advection in a fracture intersecting the disposal cell (e.g., Arcos et al. 2003, 2008; Sena et al. 2010; Benbow et al. 2019).

Perturbations from atmospheric O_2 and CO_2 during the construction and ventilation stages of the repository life constitute a particular type of interface, a physical contact with air, where the aggressive agent is a gaseous component instead of interstitial water and minerals.

The modeling of the behavior of each type of material and the relevant interfaces (Table 1) will be detailed in this chapter with a particular emphasis on the evolution of the RTM approaches and achievements over the past two decades.

MATERIALS IN PHYSICAL CONTACT WITH AIR

This "interface" is characterized by the direct physical contact between materials and air containing reactive gases (essentially O_2 and CO_2). In this situation, porous media are generally partially saturated with water and therefore fast diffusional transport of gas (four orders of magnitude faster than in water) can possibly occur into the pore network. The water saturation

Table 1. Types of material interfaces in different repository concepts (SF, bituminous, and cementitious waste are not detailed here).

Material interface	HLLW in clay formation	HLLW in crystalline formation	ILLW in clay formation
Clay–atmospheric O_2	Construction phase (disposal cell)	Bentonite handling and emplacement	Construction phase (disposal cell)
Concrete–atmospheric CO_2	Construction and ventilation phase (wells, tunnel)	Construction and ventilation phase (tunnel)	Construction and ventilation phase (wells, tunnel, disposal cell, container)
Iron–clay	Corrosion phase (metallic structure components, container)	Corrosion in bentonite after failure of copper container	—
SF–clay	SF alteration after failure of container	SF alteration in bentonite after failure of copper container	—
Glass–iron	Matrix alteration after water intrusion	—	—
Glass–(iron)–clay	Matrix alteration after container corrosion	Matrix alteration after container corrosion	—
Iron–concrete	Metallic structure corrosion (tunnel) and overpack corrosion in supercontainer (Belgian concept)	—	Container and metallic structure corrosion
Concrete–clay	Repository lifetime (wells, tunnel, disposal cell) and supercontainer in Belgian concept	—	Repository lifetime (wells, tunnel, disposal cell, container)
Glass–concrete–(clay)	Matrix alteration after container corrosion in Belgian supercontainer concept	—	—
Bituminous, cementitious, metallic waste–concrete–(clay)	—	—	Matrix alteration after container corrosion

conditions will change with time resulting from the resaturation process with water coming from the surrounding host-rock and invading the tunnels, shafts, and wells. Resaturation will be initially impeded by ventilation during the operation phase and then by the generation of gas that may accumulate in the disposal cells (mainly H_2) after closure. These two stages will produce very different geochemical environments, with contrasting reactivity, during which oxic vs. anoxic redox conditions will prevail. Long timespans with oxic conditions are to be avoided to limit the corrosion rate and to make sure reduced conditions are settled when radionuclides are released (because their oxidized forms tend to be more mobile). Calculating the duration of this stage is therefore important, but it is not thought to be very long once the disposal cell is closed (tens to thousands of years) due to the numerous oxygen consuming reactions that will occur in the vicinity of the disposal cell such as iron corrosion, dissolution of reducing mineral, and microbial respiration (see following sections).

The duration of the resaturation stage is difficult to predict because it strongly depends on the relative importance of the two counteracting processes (Marschall et al. 2005). It has been studied by conducting numerical simulations at disposal cell scale where the focus was to predict the transport and fate of hydrogen. The resaturation time calculated in the near field for different repository concepts varies in a very broad range from hundreds to hundreds of thousand years. It was found to be strongly linked to the diffusivity of dissolved hydrogen and the H_2 production rate in the HLLW cells (Xu et al. 2008; Poller et al. 2011; Senger et al. 2011; Enssle et al. 2014; Brommundt et al. 2014; Sedighi et al. 2015) and was even longer in the ILLW cells where the degradation of waste matrices is also susceptible to produce H_2 (Talandier et al. 2006; Poller et al. 2011; Avis et al. 2013). Note that flow and reactive transport in unsaturated conditions have also been extensively studied and modeled, though in a very different geological context and repository concept, in the framework of the Yucca Mountain project (USA); in this concept, the HLLW repository was envisaged in a fractured volcanic tuff formation at a depth approximately 300 m above the water table (e.g., Glassley et al. 2003; Spycher et al. 2003).

Corrosion of carbon steel components in oxic conditions

In repository conditions, metallic iron is not thermodynamically stable in the presence of water, and the corrosion of metallic iron occurs both in oxic (operation phase) and reduced conditions (post-closure period). In the first case, corrosion leads to the release of ferric iron and hydroxide in solution (Reaction 3), whereas in the second case corrosion produces aqueous ferrous iron, hydrogen and hydroxide (Reaction 4).

$$4\,\mathrm{Fe(s)} + 6\,\mathrm{H_2O} + 3\,\mathrm{O_2(aq)} \rightarrow 4\,\mathrm{Fe^{3+}} + 12\,\mathrm{OH^-} \quad (3)$$

This reaction leads either to a pH increase with an increase in redox potential or to a pH increase with a decrease in redox potential. While anoxic corrosion is often taken into account in RTM studies (see dedicated section below), oxic corrosion is seldom tackled, despite a much higher corrosion rate (Féron et al. 2008; Johnson and King 2008) and the development of more aggressive mechanisms such as pitting or crevice corrosion (Barnichon et al. 2018). This phenomenon is also observed in experiments with sequential aerobic–anaerobic conditions (Sherar et al. 2011; El Hajj et al. 2013).

There are few modeling studies dealing with corrosion during the oxic phase in the context of a disposal cell. The first attempts were dedicated to the assessment of the evolution of O_2 and H_2 content during the ventilation period using a 2D domain containing the container-EDZ-argillites system (Hoch and Wendling 2011). They used a TH(C) model where the only reaction is iron corrosion, and the model uses a water saturation-dependent formulation for the corrosion rate in oxic (consuming O_2) and anoxic (producing H_2) conditions. The results showed that oxygen diffusing from the tunnel is rapidly consumed by corrosion (with a rate ~100 µm/y) and the propagation front was limited to ~10 m (in a 40 m disposal cell). With the production of H_2 on the other side (corrosion rate of 10 µm/y), the mole fraction increased to 0.3 at the end of the cell, but the fraction of both gases reached only ~0.1 where they mixed.

In their study, De Windt et al. (2014) added the kinetics of pyrite oxidative dissolution as an oxygen consuming reaction. They first checked the robustness of their RTM approach to reproduce an in situ experiment conducted in a borehole in the Tournemire URL (France). The predicted mineralogical evolution (goethite/magnetite) qualitatively matched the *in situ* experiment. Applying the model to the repository scale, they show that the gas diffusion coefficient in the partially saturated zones plays a major role in the location of the oxidizing/reducing front inside the engineered barriers with oxic corrosion of steel on one side and anoxic steel corrosion accompanied by hydrogen production on the other side. A similar study was performed by (Bond et al. 2013), matching the sulfate concentration from pyrite dissolution in an *in situ* experiment in the Mont-Terri underground research laboratory (Switzerland).

Recent studies tend to integrate more phenomenological models to determine the corrosion rate in oxic and anoxic conditions. The oxic corrosion model takes into account the thickness of the water film on the iron surface, and the diffusion of O_2 in a goethite/lepidocrocite layer as the rate-limiting step (Hoerlé et al. 2004). The onset of corrosion happens when a critical amount of water condenses on the iron surface. The results of calculations at the disposal cell scale show in particular that corrosion concentrates in locations where the relative humidity is highest, especially where water "leaks" from fractures, with corrosion rates up to 200 µm/y locally.

Oxic transient: impact on claystone

Argillaceous rocks react with meteoric carbon dioxide (CO_2) and oxygen (O_2) from the atmosphere and nested chemical reaction fronts form in the subsurface in response to acid–base and redox reactions (Brantley et al. 2013). In a geological repository, similar phenomena will occur in the anaerobic host rock during construction (excavation, drilling operations) and operations (gallery ventilation). Under these conditions, the prevailing reducing conditions will be perturbed and redox-sensitive minerals (e.g., Fe-bearing minerals) will react. The expected chemical changes have been recently reviewed (Bildstein and Claret 2015) and the main weathering effects to be expected are recalled here. In claystone, oxidation mainly affects pyrite, which is ubiquitously found in the mineral assemblage. As it oxidizes with exposure to oxygen and water, pyrite releases sulfate and protons. The overall reaction under oxic conditions is expressed as:

$$FeS_2 + 0.5\ H_2O + 3.75\ O_2(aq) \rightarrow Fe^{3+} + 2\ SO_4^{2-} + H^+ \quad (4)$$

While the release of ferric ions causes the precipitation of iron (oxy)hydroxides, carbonates will play a major role in the buffering of proton release concomitantly affecting the population of the clay exchanger. At the laboratory scale, flow-through oxidation experiments conducted on COx tailings can be reproduced using RTM studies (Claret et al. 2018a). Recently an *in situ* experiment (OXITRAN) has been set up in the Tournemire underground research laboratory in which the time evolution of oxygen partial pressure in a measurement chamber isolated from the atmosphere has been recorded (Barnichon et al. 2018). Although pyrite is present and can buffer an oxygen plume while CO_2 is produced (Vinsot et al. 2017), oxygen was never completely depleted in the test chambers. The key controlling parameters are the thickness of the Excavated Disturbed Zone and the ratio between the effective diffusion coefficient and the oxygen consumption first-order effective rate. In contrast, the 'Full-Scale Emplacement' (FE) experiment that was initiated at the Mont Terri rock laboratory aims to simulate, as realistically as possible, the construction, waste emplacement, backfilling and early post-closure evolution of a spent fuel/vitrified high-level waste disposal tunnel according to the Swiss repository concept. First results indicate rapid oxygen consumption at locations not affected by O_2 inflow from the access tunnel (Müller et al. 2018). In addition to oxygen diffusion, drilling is also associated with desaturation and water evaporation, leading to increased salt concentration in the pore water (Zheng et al. 2008; Lerouge et al. 2013). A multiphase flow and reactive transport model of a ventilation experiment performed on Opalinus Clay indicates that changes in the clay mineral porosity caused by oxidation and the associated mineral dissolution/precipitation may seem weak (Zheng et al. 2008). The pore water seeping into the drifts and the gallery (e.g., after closure of the repository) will however interact with the oxidation products and the salts inherited by water evaporation. This more saline water will interact first with the repository materials.

Atmospheric concrete carbonation

This interface is relevant for concrete waste packages and cell structures (in most ILLW and the Belgian HLLW concepts) and for concrete components found in parts of other HLLW repositories (tunnels). Studies concerning this interface have benefited from the work that has been conducted for the atmospheric carbonation of buildings and civil engineering structures

(see Ashraf 2016, for a review). In the carbonation process, the main chemical reaction is the acid attack caused by CO_2 dissolving in water and triggering the dissolution of portlandite and the initial calcium-silicate-hydrate (C-S-H) phases to form calcium carbonate minerals (calcite, aragonite, vaterite) (Reaction 5), and new C-S-H phases with progressively decreasing Ca/Si ratio (amorphous silica being the ultimate alteration product, Reaction 6). Sulfate-bearing minerals are also affected by carbonation with the initial ettringite dissolving to form basanite ($CaSO_4 \cdot 0.5H_2O$) or gypsum ($CaSO_4 \cdot H_2O$), depending on the relative humidity.

$$\mathrm{Ca(OH)_2 + CO_2(aq) \rightarrow CaCO_3 + H_2O} \tag{5}$$

$$\mathrm{(CaO)_x (SiO_2)_y (H_2O)_z + x\,CO_2(aq) \rightarrow} \\ \mathrm{x\,CaCO_3 + y\,SiO_2 \cdot t\,H_2O + (x - t + z)\,H_2O} \tag{6}$$

The models taking into account the coupling of CO_2 diffusion in the gas phase with the drying process are of particular interest for atmospheric carbonation at the disposal cell scale. During the ventilation period, air will be forced into the tunnels at a constant, low relative humidity (~40%) at a temperature close to 25 °C (or may be slightly heated, up to 40 °C, in preliminary concepts from Andra 2005). The drying process is mainly controlled by water flow out of the concrete, the driving force being water evaporation at the surface. It can be described via full multiphase RT models or alternatively with Richards' Equation (depending on the concrete properties).

Most of the experiments conducted up to 2005 focused on carbonation "kinetics," looking for the location of the carbonation front (identifying the pH front at ~9 with the phenolphthalein test) without providing quantitative mineralogical information. These experiments were modeled with simplified chemical models (e.g., Bary and Sellier 2004; Burkan Isgor and Razaqpur 2004). Only recently have experimental studies looked more closely at mineralogical changes, starting with portlandite and calcite, then adding aragonite and vaterite (Drouet 2010; Drouet et al. 2018), and ettringite, gypsum, and basanite (Auroy et al. 2018). The first modeling work actually using RTM was proposed by (Bary and Mügler 2006) with the objective of matching the portlandite and calcite profiles observed in experiments. They used a full multiphase flow code and developed a shrinking core model for the dissolution of portlandite and precipitation of calcite with a diffusion-limited rate. They also took into account the changes in porosity and the effect on permeability (through Kozeny–Carman relationship). The model only solves for the mass conservation of water, calcium and carbonate without full chemical treatment. Modeling results reproduce the observed carbonation front and a decrease in porosity for a series of experiments for three cement types at three different liquid saturations (0.65, 0.80, and 0.95). This model was then extended to account for the complete chemistry by Leterrier and Bary (2011), but was only calibrated on the carbonation front for the same experiment. A similar modeling approach was used by (Park 2008), although without the shrinking core model.

RTM studies of concrete carbonation at the disposal cell scale are scarce, especially those covering typical ventilation times (~100 years) and coupling carbonation with concrete drying (Trotignon et al. 2011; Thouvenot et al. 2013). In these two studies, the geometries of the waste package and the tunnel structure were simplified and handled as a 1D problem. The evolution of the complete mineralogy of concrete is investigated (see dedicated section below) and the problem is treated with full multiphase flow and transport using TOUGHREACT. It includes the feedback of porosity and phase saturation on diffusion using the Millington-Quirk relationship (with specific parameters for concrete) and a slipping factor to account for the larger gas-intrinsic permeability compared to water (Thiery et al. 2007; Zhang et al. 2015). Results show that the carbonation of concrete develops over 1 to 10 cm/100 years depending on the concrete properties and that, in the carbonated zone, the primary minerals dissolve all the way to the

"ultimate" secondary minerals (calcite, amorphous silica, gypsum, gibbsite, ferric hydroxide), with no intermediate minerals (e.g., C-S-H). In contrast with previous results, porosity changes in these simulations are not significant (a few percent at most). It is noteworthy that these results are sensitive to the way the atmospheric cell in contact with concrete is implemented in codes as it has a direct impact on the flux of gaseous CO_2 entering into concrete: size of the cell, diffusive properties in the gas and the aqueous phase.

The modeling results do not integrate some of the features observed in experiments. For instance, C-S-H carbonation may overrun CH carbonation (Groves et al. 1990), which is not predicted in numerical simulations. Some portlandite also remains, even after a long time in some experiments (Drouet 2010; Auroy et al. 2018; Drouet et al. 2018). Further tests with the shrinking core model may succeed in reproducing these observations. In combination with this phenomenon, the decrease of reactivity when liquid saturation is below 0.3–0.4 has been observed (Thiery 2005; Thiery et al. 2013) and implemented by Thouvenot et al. (2013) but to calibrate such a function in codes requires more data.

Another noteworthy feature of this type of simulation is that the computing time can be quite long. For instance, due to the lack of an implicit scheme for the coupling of transport in the gas phase and RT in the aqueous phase in TOUGHREACT, the CPU time can be one to several months for 100 years of physical time (Trotignon et al. 2011; Thouvenot et al. 2013). Note that a recent development proposes an interesting "look-up table approach" for the two-phase reactive transport, which could partly help solve the simulation CPU time (Huang et al. 2018).

Finally, some important effects of carbonation on the properties of concrete that have been largely observed are not actually taken into account in modeling (Czarnecki and Woyciechowski 2015; Ashraf 2016; Savija and Lukovic 2016): changes in porosity, transport properties, micro- and macro-mechanical properties, shrinkage and cracking. Experimental data has been recently acquired on changes in water retention properties and permeability (Auroy et al. 2013, 2015, 2018). The impact of carbonation is not the same for the different types of concrete (Auroy et al. 2015), which would also constitute an interesting challenge for RTM.

THE IRON–CLAY INTERFACE

The iron–clay interface is studied in almost all countries where deep geological disposal of HLLW is envisaged. Significant amounts of metallic components (drift liner, structure, and containers) are used to ensure mechanical resistance of the waste package and to retard contact of waste matrices with water during the initial thermal stage, whereas clay barriers are used to retard RN migration. Although a variety of metallic alloys are envisaged in repositories (King and Shoesmith 2010; King 2014), the corrosion of these components in anoxic conditions is often simplified in the modeling studies into iron corrosion and takes place according to Reaction (7).

$$\mathrm{Fe(s)} + 2\mathrm{H_2O} \rightarrow \mathrm{Fe^{2+}} + 2\mathrm{OH^-} + \mathrm{H_2(aq)} \quad (7)$$

First modeling studies at the scale of the disposal cell

The first modeling studies concerning this interface attempted to implement the knowledge acquired in experiments on iron–clay interactions in deep geological conditions initially conducted in batch systems with powdered materials starting in the late 1990's (see Bildstein and Claret 2015 for a recent review). These experiments focused on understanding the processes, identifying the corrosion products (magnetite, siderite) and the secondary minerals resulting from the alteration of clay minerals (Fe-serpentine, and zeolites and Fe-chlorite at higher temperature), and quantifying the corrosion rate (in the order of 1 µm/year). The calculations presented in the study of Montes-H et al. (2005) were performed at the scale

of the bentonite barrier perturbed by a source of iron on one side and *in situ* groundwater on the other side; mineral dissolution used the kinetics law, precipitation occurred at equilibrium, looking in particular at the montmorillonite-to-chlorite conversion.

Modeling studies then turned to a geometry closer to that of a disposal cell by including the iron canister into the calculation domain, adding a full kinetics approach, and focusing on porosity change and feedback on diffusional properties (Bildstein et al. 2006). The authors obtained the first result on porosity clogging after 5 000 years at the interface with bentonite and 15,000 years in the iron grid cell at the interface with the Callovo–Oxfordian claystone.

Both studies showed converging results in terms of pH increase, Eh decrease, and mineralogical evolution, although the presence of iron in the calculation domain produced stronger changes in the second study: pH from an initial circum-neutral value to ~10.5 and Eh from an initial −200 mV down to −800 mV during corrosion.

First modeling attempts to fit batch experiment results

Because significant uncertainties in the parameters used in the previous studies were highlighted (surface area, kinetics, evolution of the corrosion rate), the first experimental study to include modeling results came early with the objective of calibrating these parameters, at least partly, by matching the mineral paragenesis and the chemical indicators (pH, Eh, iron aqueous concentration) observed in the experiments. De Combarieu et al. (2007) used a mean corrosion rate (1.4 µm/year) measured in his batch experiments at 90 °C using powdered materials and iron foils. Modeling results matched the experimental data (pH = 10.5, Eh = −700 mV, precipitation of magnetite, Fe-serpentine, and Fe-silicate) using reactive surface areas calculated based on the particle size for primary minerals and the local equilibrium assumption for secondary minerals.

In a study looking at the diffusion of iron in bentonite, Hunter et al. (2007) were the first to introduce ion exchange and surface complexation in the modeling approach, using the corrosion rate measured in their experiments at 30 °C. Simple 1D calculations were performed to model the profile of iron measured into the bentonite; matching the amount of iron required making assumptions on the diffusion coefficient, surface complexation and magnetite precipitation.

Finally, Pena et al. (2008) introduced the first attempt to model a variable corrosion rate using a semi-analytical approach, hypothesizing that corrosion is controlled by diffusion through a growing magnetite film. The authors were able to match the data reported for corrosion in bentonite in batch experiments by (Smart et al. 2006) on a time scale of 0.5 year using a solid phase diffusion coefficient of 10^{-20} m^2/s for the Fe^{2+} and 10^{-19} m^2/s for H_2, H_2O, and OH^- species.

A decade of RTM evolution of simulations at the scale of the disposal cell

Later, a long series of modeling studies came back to the scale of the disposal cell; see review in Claret et al. (2018a) for a detailed description of the modeling set-up of the different studies.

While the previous studies focused on corrosion rate and mineral paragenesis, the subsequent studies at the disposal cell put the focus on full ion exchange and surface complexation with proton and Fe^{2+} (Samper et al. 2008; Wersin et al. 2008). While a 1D grid is used by Wersin et al. (2008) for the iron-bentonite system, the first 2D-axisymetric calculations are proposed by Samper et al. (2008) with an application to the iron–bentonite–granite system. Note that in both studies, the mineralogical system is simplified (no reactivity for clay minerals) and a constant corrosion rate is used in both cases, the emphasis being put on the role of sorption. The results show the importance of the surface protonation of bentonite, which reduces the pH increase during corrosion (from 11 to 9 in the bentonite), and a decrease of porosity in bentonite. The mass balance of iron shows that the precipitation of magnetite, and to a lesser extent siderite, accounts for most of the iron immobilization (iron sorbed on complexation surface is anecdotal). Note that

Samper et al. (2008) introduced an interesting "progressive", cell-by-cell, corrosion process. This is also the first study to perform a thorough sensitivity analysis of uncertain parameters (corrosion rate, protonation sites, and surface complexation vs. exchange of Fe^{2+}).

In a series of simulations with a constant corrosion rate, Savage et al. (2010) tried to tackle the tricky issue of the long-term evolution of the Fe-minerals in the mineralogical assemblage in the iron-bentonite system by using evidence for mineral parageneses from analogous natural systems. They allowed for faster minerals to precipitate initially and other more stable minerals to take over through nucleation and Oswald ripening, based on the early work of (Steefel and Vancappellen 1990). This is the only work where the authors were able to describe a magnetite → cronstedtite → berthierine → chlorite mineralogical sequence at the iron–clay interface over a period of 1 My (according to experimental results reviewed by Mosser-Ruck et al. 2010).

It was only a couple of years after the first attempt to develop a model corrosion rate depending on the chemical environment by Peña et al. (2008), that non-constant iron corrosion rates were introduced in large-scale calculations, and to date only Wilson et al. (2015) have implemented a corrosion rate controlled by diffusion. In most other cases, a simpler model was adopted, in the form of a "standard" rate law, i.e. with a term considering the departure from equilibrium considering reaction (3). This assumption results in a progressive decrease of the corrosion rate, usually by an order of magnitude over a period of 100 000 years (Marty et al. 2010; Lu et al. 2011; Ngo et al. 2014). Note that a decrease of the corrosion rate is also achieved, to some extent, by considering that the reactive surface area depends on the amount of iron and on porosity (Bildstein et al. 2006; Savage et al. 2010; Wersin and Birgersson 2014). Interestingly, in most of these studies (except Lu et al. 2011 and Wilson et al. 2015), ion exchange and surface complexation were not included in the calculations. This choice was motivated either by the fact that the focus was put on other processes (mineralogical changes, effect of transport), or because explicit surface reactions were considered to create mass by double-counting the counter ions when the mineral-bearing surface sites dissolves away in significant amounts (see sensitivity analysis in (Bildstein et al. 2012). This problem was recently treated by creating specific thermodynamic data for surface-bearing minerals to reconcile ion exchange and dissolution/precipitation processes (Benbow et al. 2019). However, note that very few data exist for surface reactions at temperature higher than 25 °C, which undermines the robustness of the interpretation.

Non-isothermal calculations were introduced into simulations quite recently by imposing a variable temperature field calculated by a TH code (Bildstein et al. 2012) or using a full THC modeling tool (Samper et al. 2016; Mon et al. 2017). This additional feature usually tends to stiffen the calculations, because RT processes and temperature are not implicitly coupled and temperature changes affect both the reactive processes (creating a thermodynamic disequilibrium and modifying kinetics) and transport.

Table 2 provides a synoptic view of the results of these studies and shows that the most abundant corrosion product predicted by the models in the long term is magnetite, sometimes with Fe-carbonates (siderite), and Fe-silicates (greenalite), sometimes incorporating Al (berthierine, cronstedtite). Primary minerals in clay are often destabilized in favor of Fe-phyllosilicates or zeolites if they are allowed to precipitate. Numerical studies often differ on the precise nature of the secondary minerals. The transformation of clay minerals into Fe-chlorite, and the timing, very much depend on whether (i) it is included as a secondary mineral, in which case it is the most stable phase and precipitates from the beginning of the simulation (e.g., Marty et al. 2010, or (ii) it results from a ripening process, taking the place of a precursor mineral in Savage et al. 2010). One of the most sensitive parameter remains the corrosion rate. The extent of the perturbation is always predicted to be limited to a few centimeters, up to 20 centimeters into the clay barrier.

Table 2. Recent RTM studies at the disposal scale with salient results.

Interfaces	Maximal perturbation extent	Main corrosion products	Main secondary minerals	Ref.
Iron–bentonite (100 °C)	(not explicit)	(not explicit)	Chlorite	[1]
Iron–claystone Iron–bentonite (50 °C)	5 cm 5 cm	Magnetite, cronstedtite clogging after 16,000 y clogging after 5,000 y	Chamosite, Fe-smectite, scolecite, Ca-zeolite	[2]
Iron–bentonite (100 °C)	7 cm	Magnetite	Fe^{2+} exchange only	[3]
Iron–bentonite (100 °C)	few cm	Magnetite	Cronstedtite, berthierine	[4]
Iron–bentonite (100 °C)	15 cm	Magnetite clogging after 100,000 y	Fe-chlorite, Fe-saponite	[5]
Iron–bentonite (^{T} not explicit)	(not explicit)	Magnetite → croenstedtite → berthierine → chlorite	Berthierine, cronstedtite	[6]
Iron–bentonite (25 °C)	(not explicit)	Magnetite	Siderite	[7]
Iron–claystone (variable *T*)	20 cm	Magnetite (Ca-siderite, greenalite)	Vermiculite, saponite, pyrrhotite	[8]
Iron–claystone Iron–bentonite (100 °C)	15 cm 10 cm	Magnetite	Greenalite, Fe-saponite, Fe-chlorite, bethierine	[9]
Iron–bentonite (25 °C)	2 cm	Test cases with only $Fe_3(OH)_7$, $Fe(OH)_2$, goethite or magnetite	Na-phillipsite, chabazite, berthierine	[10]
Iron–bentonite (70 °C)	2 cm	(not explicit)	Berthierine, greenalite, Fe-saponite	[11]
Iron–bentonite (variable *T*)	up to 14 cm	Magnetite	Fe-phyllosilicates, zeolites	[12]
Iron–bentonite (variable *T*)	1 cm	Magnetite	Brucite, gypsum	[13]

References

[1] Montes-H et al. 2005 [2] Bildstein et al. 2006 [3] Samper et al. 2008 [4] Wersin et al. 2008 [5] Marty et al. 2010 [6] Savage et al. 2010 [7] Lu et al. 2011 [8] Bildstein et al. 2012 [9] Ngo et al. 2014 [10] Wersin and Birgersson 2014 [11] Wilson et al. 2015 [12] Samper et al. 2016 [13] Mon et al. 2017.

Concerning porosity clogging, a major assumption was made in some simulations: because the phenomenology is not known when porosity vanishes, porosity update was disabled in order to reach the end of the corrosion stage (~50,000 years) (Bildstein et al. 2012). A complete inhibition of the corrosion process has never been observed in experiments, even if a dense corrosion product layer is often identified. In addition, the ubiquity of magnetite in simulation results as the dominant

corrosion product in the long term is questioned by many experimental results and archeological analogs. These issues, along with recent experimental work (Martin et al. 2008; Bourdelle et al. 2014, 2017), motivated the modelers to come back to modeling experimental results.

A recent return to modeling experimental results

Two of the most recent modeling studies revisited interactions at the experimental scale to refine the understanding and modeling of this interface. In the first work, Ngo et al. (2015) modeled iron-COx claystone interaction results obtained from the batch experiment with powdered material at 90 °C for 90 days (Bourdelle et al. 2014). Using a mean corrosion rate (determined from the experiment), standard and diffusion-controlled kinetics for mineral dissolution, and the local equilibrium assumption for precipitation, they were able to match the low pH (value ~7) and the evolution of aqueous species concentrations. They also matched the set of secondary minerals observed at the end the experiment: Ca-saponite, and greenalite. Interestingly, no magnetite was observed or simulated in these conditions. This particular feature, also observed by Bourdelle et al. (2017), was attributed to the high reactive surface area in the powdered system, producing a high precipitation rate for greenalite in the experiment (and matched by the modeling with equilibrium precipitation). Note that the simulation also predicted the transient precipitation of chukanovite, a Fe-hydroxyl-carbonate recently observed in experiments (Schlegel et al. 2010) and archeological analogs (Saheb et al. 2012), which disappears after the corrosion stage to form Ca-saponite.

In the second study, the modeling of iron corrosion in a Callovo–Oxfordian claystone block (machined from a core plug) at 90 °C for 2 years (Martin et al. 2008) was conducted by Bildstein et al. (2016). The objective was to reproduce the mineralogical paragenesis identified by (Schlegel et al. 2014) using the evolution of the corrosion rate measured in the experiment using electrochemical impedance spectroscopy (from 100 to 0.1 µm/year). The sequence of minerals observed from the contact with iron towards the claystone was as follows: magnetite, Fe-silicate, and Ca-siderite. This sequence could not be matched with the standard simulation setup (typical parameters for mineral dissolution and precipitation kinetics data, evolution of diffusion coefficient using Archie's law). The sensitivity analysis performed on the kinetic parameters (quartz dissolution, precipitation) was unsuccessful in generating the correct sequence. It was particularly difficult to maintain magnetite at the iron surface as the corrosion rate decreased with time. The observed mineral paragenesis could only be reproduced by using a cell-by-cell corrosion process and by attributing very slow diffusional transport properties to pre-corroded cells (i.e. by using a large value for the cementation factor). This layer "isolated" the iron surface from the claystone, allowing specific chemical conditions to develop at this location favoring magnetite precipitation.

The RTM simulations of iron corrosion will evolve in the short future to integrate more phenomenological corrosion models that calculate the evolution of the corrosion rate as a function of the geochemical conditions. Such electrochemical corrosion models have already been developed (Bataillon et al. 2010; King et al. 2014) and have to be coupled to RTM codes. This approach will be useful to simulate and interpret the existing laboratory experiments and also *in situ* results obtained recently (Necib et al. 2016; Schlegel et al. 2016, 2018).

THE CLAY CONCRETE INTERFACE

A brief materials mineralogy overview and associated chemical gradient at the materials interface

Before dealing with the interaction between clay and concrete, it might be interesting to recall briefly the mineralogy of these two materials. In a deep geological disposal, clay materials can be the clay-rock itself where clay minerals are the main constituents of these

rocks, but also the bentonites used for the construction of engineered barriers (Sellin and Leupin 2013). The mineralogy of clay-rocks is complex, meaning that its clay fraction not only contains pure clay mineral end-members, such as kaolinite, smectite and illite, but also mixed layer minerals (Claret et al. 2004). In addition, carbonate minerals with a range of chemical compositions and structures are present (see for example (Lerouge et al. 2013), and pyrite, along with organic matter and quartz (Gaucher et al. 2004a; Jenni et al. 2014; Zeelmaekers et al. 2015). Proportions of total phyllosilicates, carbonates, quartz, pyrite and organic matter can be found in the literature for various clay formations (e.g., Opalinus Clay, Boom Clay, Callovian-Oxfordian formation, and Boda Clay, in Altmann et al. (2012)) and can be very different from bentonites (e.g., Ufer et al. 2008; Savage and Cloet 2018).

The mineralogical composition of cementitious materials is also complex. Concrete is a composite material made of a porous matrix (the hydrated binder) filled with water, into which are embedded filler materials such as quartz and calcite, which act as a granular skeleton. As the hydration reaction proceeds due to the cement–water interaction, the anhydrous phases, calcium silicates (C3S or C2S) and calcium aluminates (C3A and C4AF) are converted into hydrates such as portlandite, C-S-H (calcium silicate hydrate), ettringite, monosulfate or monocarbonate. This decreases the bulk porosity, since the molar volume of the hydrates is much larger than that of the anhydrous phases (Van Damme et al. 2013; Gaboreau et al. 2017; Claret et al. 2018b). Concrete has a long history that began in the pre-Roman age, and its formulation, which was greatly improved at the beginning of nineteenth century with the invention of Portland cement, has recently become more and more sophisticated. Within the framework of nuclear waste disposal, such sophistication has been introduced with the development of low alkaline concrete (Codina et al. 2008). The idea behind this development was to improve concrete compatibility with the repository environment, yet it remains a high-strength concrete. On one hand, low alkaline concrete (often called "low pH" cement) has a lower alkali content than that of ordinary Portland-based cement material, which may reduce the pH gradient at the interface and therefore the changes in clay in contact with the concrete. On the other hand, it has a low-heat hydration temperature, which minimizes the microcracking that can have negative consequences on cement's long-term durability. One must also keep in mind that whatever the formulation, the hydration of cement-based material is kinetically driven, and thus the composition of its pore water evolves with its curing time.

While the measured pH in concrete is in the range 10.4 to 13.6 depending on time and formulation (Lothenbach and Wieland 2006; Luke and Lachowski 2008; García Calvo et al. 2010; Lothenbach 2010; Bach et al. 2012; Lothenbach et al. 2012, 2014), the pH of pore water in clay materials is generally in the range of 7 to 9 (Bradbury and Baeyens 2003, 2009; Wersin 2003; Bildstein and Claret 2015; Lerouge et al. 2018). Therefore, even for low-pH concrete material, the pH difference at the interface may be as much as two pH units. When the pH is above 13, the alkali (Na^+, K^+) concentrations in pore water are higher in cement material than in clay-rocks. The reverse is true for K^+ when the cement material is made of low-pH cement. Still, in relation to the pH values, partial CO_2 pressures are far lower in cement materials than in the pore water of clay-rocks, where partial pressures of CO_2 that are higher than the atmospheric pressure (~10^{-3} to ~10^{-2} bars) are reported (Gailhanou et al. 2009; Lassin et al. 2016). Redox conditions are reducing in both claystone (Brendler et al. 2003) and in reinforced steel cement materials (Aréna et al. 2018). Nevertheless, in the latter, a strong Eh gradient exists from the steel surface outward to the bulk concrete. As described just above, a steep geochemical gradient exists at the clay–concrete interface. In the 90's, early calculations based on mass balance assumptions only, and reported in Gaucher and Blanc (2006) and Savage et al. (2007), led to the conclusion that 0.2–1 m^3 of bentonite are needed to buffer the chemical perturbation created by 1 m^3 of concrete. If true, this conclusion would have been problematic for the storage concepts that rely on the properties of unaltered clay materials, and this explains why so much effort has been put in reactive transport modeling studies of both experiments that mimic clay–concrete interfaces and the long-term evolution of clay–concrete interfaces.

Reactive transport modeling of laboratory and in situ scale experiments

Before their use for large-scale simulation and long-term evolution, reactive transport models and computer codes have to be tested against experimental data in order to test and improve their robustness. Experimental data can be obtained in the laboratory with experimental apparatus that mimic storage situations (e.g., column experiment), *in situ* to better reproduce field conditions (this is possible thanks to many underground research laboratories that are in operation) or gathering data from natural analogs for which hydrogeology and geochemical conditions reproduced phenomena that are expected in the repository. In Table 2, reactive transport studies that are compared against experimental data dealing with clay–concrete interaction are reported. The focus of our chapter is claystone, which is why experimental studies that deal with high-pH plume but in granite (e.g., (Soler 2003; Pfingsten et al. 2006; Soler and Mader 2007)) have not been reported here. In addition, when some geochemical modeling is made without coupling chemistry and transport (e.g., Lalan et al. 2016) these references are also not mentioned as the focus is on reactive transport. Among the thirteen references discussed in Table 2, three deal with column laboratory experiments (two focusing on the same experiment), four are *in situ* experiments and four focus on the same natural cement analog. The latter is the Maqarin natural analog in the north of Jordan (Khoury et al. 1985; Alexander et al. 1992; Khoury et al. 1992; Chaou et al. 2017). In this area, hyperalkaline groundwater compositions are the product of low-temperature leaching of an assemblage of natural cement minerals produced as a result of high-temperature/low-pressure metamorphism of marls (i.e. clay biomicrites) and limestones. On the hydraulic downstream of the cement zone, alkaline groundwaters circulated through fractures within the biomicrite clay. On the edge of the fractures, calcite, kaolinite, silica, low amounts of illite, albite and organic matter dissolved. Within the fractures, different opening/clogging stages may have occurred, leading to a complex mineralogical pathway. Two of the modeled cement claystone interfaces were sampled during the Cement–Opalinus Clay Interaction (CI) Experiment at the Mont Terri rock laboratory (Jenni et al. 2017). This is a long-term passive diffusion-reaction experiment between contrasting materials of relevance to engineered barrier systems/near-field for deep disposal of radioactive waste in claystone (Opalinus Clay). The sampled interfaces have been (and are still) extensively characterized from the mineralogical and petrophysical point of view (Jenni et al. 2014, 2017; Dauzeres et al. 2016; Lerouge et al. 2017). The two other *in situ* interfaces were sampled in the Tournemire underground research laboratory. Again, these interfaces have been extensively investigated (Tinseau et al. 2006; Gaboreau et al. 2011; Bartier et al. 2013). In one of the column laboratory experiments, bentonite was exposed on one face to a solution that mimic cementitious pore water, while the opposite face was a homo-ionization solution. In the second, concrete and bentonite plugs were juxtaposed. For the column laboratory experiments, heat was applied either in isothermal conditions (60 °C or 90 °C) or by applying a thermal gradient. These are the only studies in where temperature plays a role. Except for (i) the hydration concrete-bentonite column test, where non-saturated conditions and thermal gradients imply the use of a THMC coupled model, (ii) the natural cement analog and one *in situ* experiment where fractures play a role, a diffusive regime was the main dominant transport process in all other experiments. The column experiments and *in situ* experiments were sized in the 10 cm range, whereas for the Maqarin natural analog site a ~100 m fracture was considered in simulation, but matrix diffusion perpendicular to the fracture was in the 10 cm range. In most of the publications described in Table 2, the thermodynamic data used come from existing databases that are either merged together (i.e. a clay-oriented database with a cement-oriented database) or completed with some missing data (e.g. zeolite, M-S-H). Depending on the reactive transport code used, the C-S-H representation is made either by considering a discrete calcium to silica ratio (e.g. 1.6, 1.2 and 0.8), or by considering a jennite-tobermorite solid solution. The latter approach was used for the studies that used GEM (Wagner et al. 2012; Kulik et al. 2013) for the reactive part. The main findings

Table 2. Review of the experiments that mimic clay/concrete interaction and that have been modeled using reactive transport modeling.

Experiment	Main conclusion	Ref.
Mineral fluid interactions occurring at the Maqarin site in Jordan (natural cement analog)	In qualitative agreement with observations at the Maqarin site, the simulations predicted that ettringite with lesser amounts of hillebrandite and tobermorite are the dominant alteration products formed at the expense of the primary silicates in the rock matrix and fracture. Depending on the rate constant for secondary mineral precipitation reactions (either the same in both the rock matrix and fracture or one order of magnitude higher in the fracture compared to the rock matrix), the simulations suggested two possible scenarios for porosity reduction (either the matrix first or the fracture first).	[1]
	Simulations indicated that the pore clogging caused by precipitation of ettringite and C-S-H minerals occurred after several hundred years at a distance of 5–10 mm from contact with the hyper-alkaline solution. Sensitivity analysis shows that clay minerals controlled the availability of Al, which is needed for ettringite and C–S–H phase precipitation. Therefore, temporal evolution of porosity changes was controled by clay dissolution.	[2]
	Major secondary minerals (e.g., ettringite, C-S-H) were controlled by the dissolution of primary silicates. Extension of porosity reduction along the fracture and in the fracture-wall rock interface depended on assumptions regarding flow velocity and composition of the high-pH solution.	[3]
	RTM predicted that ettringite, thaumasite, jennite and tobermorite dominate the fracture filling materials. Alteration of the marl led to scolecite, ettringite, C-S-H and a small amount of sepiolite. If an armored layer was considered in the fracture, only calcite and jennite precipitate. Fracture sealing is complex.	[4]
For about 2 years, a cylindrical compacted bentonite column was in contact with a 0.6 $MgCl_2$ solution and either a young cement water (YCW, pH = 12.4 at 60 °C) or an evolved cement water (ECW, pH = 11.5 at 60 °C)	Major mass transfer and mineral transformation pathway (including the diffusion of alkaline cations through ion exchange reaction) experimentally observed were reproduced by RTM. For the most reactive system (YCW), partial dissolution of montmorillonite and precipitation of Mg-Silicate, hydrotalcite and brucite were predicted	[5]
	In this case modeling was blind because it was done prior to the experiment. The model reproduced well the porosity decrease induced by secondary mineral precipitation as well as ion exchange. The kinetic dissolution model played an important role in the outcome of the simulations.	[6]
Two cylinders of bentonite and concrete were put into contact for 54 months in hermetic cells that allowed both heating up to 100 °C on the bottom (bentonite side) and water circulation on the top.	On-line measured temperature, relative humidity data, water content and porosity data were well reproduced by the THMC model. Except for ettringite and C-S-H phase, for which the predicted precipitation was smaller than experimental data, RTM captured the main trend of the mineralogical pathway. Increasing the specific surface area of ettringite improved the model.	[7]

Table 2 (cont'd). Review of the experiments that mimic clay/concrete interaction and that have been modeled using reactive transport modeling.

Experiment	Main conclusion	Ref.
A 15-year in situ claystone /Ordinary Portland Concrete (OPC) interface was sampled in the Tournemire Underground Research Laboratory	While profiles calculated at local equilibrium or using kinetics are very similar in concrete, kinetics really improved the representation of experimental data in the claystone. Mineralogical transformation simulated in the claystone matrix and in the fracture filling were quite comparable as observed on the field. C-S-H, ettringite and carbonates (predominance of metastable vaterite over calcite) were modeled at the OPC/claystone interface, followed by a zone of clay-likes phases and calcite and a last zone with precipitation of calcite (going deeper in the fracture).	[8]
An eighteen-year in situ experiment putting CEM II and Toarcian claystone in contact at Tournemire Underground Research Laboratory was dismantled, analyzed and modeled.	RTM was used to test one hypothesis, namely the introduction of a sedimentary fluid into the macroporosity of the cement paste to explain the formation of part of these secondary phases. Simulations indicate that such transport could have occurred near the argillite/cement paste contact at a very early stage. After this stage, the transport was reversed and "cementitious" fluids flowed from the cement paste to the argillite. Experimental observations of C-S-H neoformation in the claystone, carbonate formations at the interface were well reproduced by simulation.	[9]
Five and 2.5-year in situ interaction of two different low-pH cements (ESDRED and LAC) with Opalinus Clay (OPA)	RTM corroborated calcite precipitation, C-S-H decalcification and M-S-H formation at the interface.	[10]
Five-year in situ interaction of Ordinary Portland Cement (OPC) with Opalinus Clay (OPA)	RTM reproduced well the decalcification of the cement at the interface, the Mg enrichment in OPA detached from the interface and the sulfur enrichment in the OPC detached from the interface.	[11]
Six-year interaction between a hardened Portland cement and water-conducting shear zone. In situ experiment conducted at the Grimsel Test Site in Switzerland	Two RTM models were used, one in 1D and one in 2D. They did not properly represent all the concentration evolutions as a function of time. However, the main parameters like pH and Ca were captured. Both models evidenced dissolution of the fault gouge minerals. The 2D model indicated an associated secondary mineral precipitation and a porosity reduction. Ettringite, C-A-S-H, and hydrotalcite also precipitated.	[12]
	In comparison to Chaparro et al. (2017), a 3D model was used here. Although some elements' concentration as a function of time (like Mg) were poorly reproduced, RTM captured the essential features of the cement leaching (e.g., portlandite dissolution) and carbonate mineral precipitation. In addition, the model results highlighted uncertainties surrounding cement solid dissolution rates and rates of secondary mineral formation.	[13]

References
[1] Steefel and Lichtner 1998 [2] Shao et al. 2013 [3] Soler 2016 [4] Watson et al. 2016 [5] Fernandez et al. 2010 [6] Watson et al. 2009 [7] Samper et al. 2018 [8] De Windt et al. 2008 [9] Bartier et al. 2013 [10] Dauzeres et al. 2016 [11] Jenni et al. 2017 [12] Chaparro et al. 2017 [13] Watson et al. 2018

and conclusions of the various studies are given in Table 2; therefore, they will not be detailed in the text. However, general conclusions can be drawn. Although some discrepancies between models and experiments could appear because new or completed datasets become available after modeling (Chaou et al. 2017), reactive transport modeling shows a great capability for reproducing the experiments (e.g., mineralogical transformation pathway and clogging processes). It is also a very useful tool for performing sensitivity analyses of input parameters and testing hypotheses. One of the most critical parameters that has been described in reported studies deals with kinetics and reactive surface areas that can play a large role in sequential minerals' appearance or disappearance, as well as the localization of porosity reduction.

Reactive transport modeling of the long-term evolution of clay–concrete interfaces

As previously stated, reactive transport modeling is a powerful tool for describing and reproducing phenomena that occur at both the time and space experimental scale. However, these scales are at least four or five orders of magnitude lower than the one we have to deal with for the long-term evolution of clay–concrete interfaces with geometries that are relevant for the repository gallery scale. In that case, reactive transport models are used to bridge the scale and make predictions about long-term evolution. Our literature review (which might not be fully exhaustive) found about twenty reactive transport studies addressing these issues during the past two decades (Table 3). In these studies, anionic exclusion in clay and multi-components diffusion were not considered. The complexity of the phenomena that were modeled lay more in considering an exhaustive mineralogy and steep chemical gradients that are not always easy to handle from a numerical point of view, even for modern reactive transport codes. The number of reactive transport codes used was also considerable: PRECIP (Savage et al. 2002), GIMRT (Lichtner 1996), HYTEC (van der Lee et al. 2003), PHREEQC (Parkhurst and Appelo 1999),TOUGHREACT (Xu et al. 2004 ; Burnol et al. 2006), ALLIANCES (PHREEDC/MT3D, (Montarnal et al. 2007), CORE^{2D} V4 (Samper et al. 2003), CRUNCH (Bildstein and Claret 2015), OpenGeoSys-GEM (Kolditz et al. 2012), ORCHESTRA (Meeussen 2003), MIN3P-THCm (Mayer et al. 2002). A detailed description of most of the above-mentioned codes and their history can be found in Steefel et al. (2015b). Many databases have also been used: EQ3/6 (Wolery 1983), CEMDATA2007 (Lothenbach and Wieland 2006; Lothenbach and Winnefeld 2006), Nagra/PSI database (Hummel et al. 2002), THERMOCHIMIE (Blanc et al. 2015a,b), THERMODDEM (Bartier et al. 2013). The geometries (1D or 2D Cartesian, 1D radial, 1D or 2D axisymmetric and 2D with cylindrical coordinates), the mesh size (usually in the cm range), the transport parameters, the way mineral dissolution or precipitation was accounted for (either at local equilibrium and/or in kinetics) have been recently reviewed (Claret et al. 2018b). Otherwise, in the case of the mass balance calculations reported earlier in this chapter, all reported studies are consistent with very limited spatial extension, in terms of mineral precipitation and dissolution, of cement perturbation in clay materials and vice versa. Not all the reported studies consider exactly the same starting mineralogical assemblages, the same secondary potential mineral phases, the same transport properties, or the same geometries (see (Table 3). This is inherent to the starting conceptualization, but also to the quality and completeness of the databases that have been improved with time, as well as the code capability. For example, in earlier calculations, cement material was not represented as a porous medium but rather as an alkaline plume imposed as a boundary condition on one side of the clay domain. Therefore, in order to evaluate the impact of different modeling assumptions among available studies, Marty et al. (2014) carried out calculations with a consistent set of data and input parameters arranged with increasing order of complexity (e.g., the considered geometry, the representation of porous media, the choice of secondary minerals phases). This standardized approach allowed for a proper comparison of numerical results and showed that modeled reaction pathways were mostly independent of the modeling assumptions for simulations carried out in the presence of water-saturated conditions. To compare the results of the various simulations after 100,000 years, concrete and clay degradation indicators were selected. In the concrete zone, the simulations were

Table 3. Review of the experiments that mimic clay/concrete interaction and that have been modeled using reactive transport modeling.

Interfaces	Maximal perturbation extent	Main mineralogical changes	Ref
Hyperalkaline fluids-bentonite (25 and 70 °C)	60 cm after 1000 yr	C-S-H neoformation close to the interface, while zeolites and sheet silicates precipitate further away. Some growth of primary bentonite minerals (analcime, chalcedony, calcite and montmorillonite) was observed under certain conditions. Porosity clogging.	[1]
Hyperalkaline fluids fractured marl (25 °C)	6 m along the fracture after 5000 yr for the higher pH	Replacement of dolomite by calcite and precipitation of secondary minerals such as brucite, sepiolite, analcime, natrolite and tobermorite led to decreased porosity in the fracture.	[2]
Ordinary Portland cement-Toarcian claystone (25 °C)	Depends on the selected minerals but alkaline plume is a buffer close to the interface	Close to the interface portlandite dissolution, C-S-H, brucite (hydrotalcite) precipitation, while further on, the interface dolomite dissolve and calcite precipitate. Depending on the hypothesis, precipitation of secondary phases such as illite and zeolite might occur. Clogging occurs after 2500 years in the claystone, whereas porosity increases in the concrete at the interface.	[3]
Waste pckage-MX80 bentonite-Portland cement liner/wall-OPA claystone	1 m in bentonite and 0.5 m in cement after 100,000 yr	Portlandite dissolution with sequential precipitation of C-S-H with decreasing Ca/Si ratio. Precipitation of brucite, calcite, hydrotalcite and illite in relatively low concentrations. Montmorillonite is almost unaltered whereas kaolinite and quartz are partly dissolved. Change in the exchanger population.	[3]
Hyperalkaline fluids-COx claystone (25 °C)	70 cm after 100,000 yr	First a change in the exchanger population (Na is replaced by K and then by Ca) occurs. Then illitization of the montmorillonite occurs. Between the illitized zone and the concrete interface, zeolite phases precipitate. Finally, cement phases (e.g. tobermorite, ettringite) replace zeolites at the concrete interface leading to porosity reduction.	[4]
Portland concrete-COx claystone Non isothermal and non-saturated condition		Tobermorite precipitation induced porosity clogging after 900 yr. In concrete, hydrogarnet and portlandite dissolve and monosulfoaluminate is transformed into ettringite. In clay, dolomite is replaced by calcite while illite and a calcic saponite are precipitating to the detriment of montmorillonite and quartz.	[5]
CEM I/ CEM V cement paste-either interstitial COx pore water or claystone (25 °C)	1.3 m after 400,000 yr for CEM I 0.2 m after 400,000 yr for CEM V	For CEM I, the porosity reduction is driven by zeolites, illite, quartz and calcite precipitation. For CEM V, secondary smectite and calcite precipitation are described.	[6]

Table 3. (cont'd). Review of the experiments that mimic clay/concrete interaction and that have been modeled using reactive transport modeling.

Interfaces	Maximal perturbation extent	Main mineralogical changes	Ref
Bentonite–concrete-Callovo Oxfordian claystone (25 °C)	Not explicit	Portlandite dissolution and C-S-H precipitation. In clay, an exchange reaction (Ca replacing Na) is observed. Montmorillonite dissolved but remains despite the alkaline plume	[7]
Portland cement-either interstitial CO*x* pore water or claystone 25 °C	Less than 2 m after 100,000 yr	Cement–interstitial CO_x porewater: Portlandite dissolution, reduction of Ca/Si ratio in C-S-H. Calcite, brucite, sepiolite and hydrotalcite representing the final stage of cement alteration. Cement–CO_x: Portlandite dissolution, reduction of Ca/Si ratio in C-S-H (jennite to tobermorite), ettringite, hydrogarnet and brucite precipitate. Dissolution of illite and montmorillonite and tobermorite and zeolite precipitation. Both porosity opening and reduction depending on the position from the interface and time. Mg speciation and illite and quartz kinetic parameters are key parameters.	[8]
Bentonite–concrete–claystone 25 °C	~30 cm in both concrete and clay side	Dissolution of primary silicate minerals (e.g. montmorillonite and quartz) and precipitation of saponite, phillipsite, illite and calcite. In concrete, portlandite dissolution, Ca/Si ratio decrease in C-S-H, ettringite precipitation. Porosity clogging localization and appearance times depends on the modeling assumption (local equilibrium, kinetic rates).	[9]
Portland cement–FEBEX bentonite 80 °C	few cm after 100 000 yr	Precipitation of hydroxides, zeolites secondary clay minerals and cement hydration phases (e.g. C-S-H) in bentonite.	[10]
Portland cement–CO*x* claystone 25 °C	~30 cm in both concrete and clay side	Dissolution of primary silicate minerals (e.g. montmorillonite and quartz) and precipitation of saponite, phillipsite, illite and calcite. In concrete, portlandite dissolution, Ca/Si ratio decrease in C-S-H, ettringite precipitation. Porosity clogging localization and appearance times depends on the modeling assumption (local equilibrium, kinetic rates).	[11]
CEM I cement–CO*x* claystone	Non isothermal, non saturated conditions	Portlandite dissolution and calcite precipitation. C-S-H with Ca/Si=1.6 dissolution and katoite precipitation. Brine formation and salt (e.g. syngenite, burkeite) deposition in the parts of the concrete where drying occurs.	[12]
Bentonite-ESRED "low pH" concrete–OPA claystone 25 °C	Few tens cm both in ESDRED and OPA or less 10 cm at bentonite-ESDRED interface	In bentonite, the main mineralogical transformations are the precipitation of calcite and hydrotalcite and the replacement of the [Na,Mg]-montmorillonite by a [Ca,K]-montmorillonite. In OPA claystone, two alteration regions are observed (inclusion of clogging). Very close to the interface, kaolinite and illite are transformed into a substitute for smectite-like phases. Depending on the coordinate in space and time, quartz, calcite and pyrite may dissolve, but partial neo-formation of calcite and illite is also possible. In the concrete liner zone close to the interface, the complete degradation of the low Ca/Si-ratio C-S-H phases is predicted, accompanied by the precipitation of hydrotalcite, zeolites, clay minerals, gypsum and calcite.	[13]

Table 3. (cont'd). Review of the experiments that mimic clay/concrete interaction and that have been modeled using reactive transport modeling.

Interfaces	Maximal perturbation extent	Main mineralogical changes	Ref
OPA or Effingen Member or Palfris formation-CEM I concrete 25 °C	10 cm in claystone 20 cm in concrete (depends slightly on the considered claystone)	Montmorillonite and portlandite dissolution. In claystone, phillipsite (Na, K or Ca), illite, calcite, hydromagnetite, hydrotalcite precipitation. In concrete, C-S-H, ettringite, calcite precipitation. Clogging occurs in all cases.	[13]
Portland cement-Interstitial Boom clay pore water 25 °C	Few mm	Portlandite dissolution, Ca/Si ratio decreases in C-S-H. Dissolution of AFm and Aft. Large amount of calcite precipitation leads to the clogging of porosity.	[14]
Hyperalkaline fluid/ Portland cement-COx claystone	Depends on the selected indicators and the scenario (from m to cm range)	In the concrete, zone alteration front is followed based on portlandite and ettringite dissolution, while in claystone dolomite, montmorillonite are used.	[15]
CEM I concrete-COx claystone	Not explicit	Interest of the paper lies in the benchmark. All codes described the same minerals paragenesis at the interface as well as clogging.	[16]
Cement backfill-Groundwater (2) representative of crystalline rock		For the higher ionic strength (0.48 mol/kg), cement alteration (e.g. hydrogarnet) led to sulfate-rich and chloride-rich solid (e.g. Friedel's salt) precipitation, along with some brucite forming and pore clogging after 78 years. In contrast, the lower ionic strength (0.005 mol/kg) led to leaching and the precipitation of calcite, along with saponite, and minor amounts of ettringite, with pore clogging taking 531 years. Thaumasite could also be a byproduct of sulfate attack on the cement.	[17]

References

[1] Savage et al. 2002 [2] Soler 2003 [3] De Windt et al. 2004 [4] Gaucher et al. 2004b [5] Burnol et al. 2006 [6] Trotignon et al. 2006 [7] Montarnal et al. 2007 [8] Trotignon et al. 2007 [9] Yang et al. 2008 [10] Fernandez et al. 2010 [11] Marty et al. 2009 [12] Trotignon et al. 2011 [13] Berner et al. 2013 [14] Ferrand et al. 2014 [15] Blanc et al. 2015b [16] Marty et al. 2015b [17] Watson et al. 2018

compared by examining both the total portlandite-dissolution (accounting for both hydrolysis and carbonation) and (ii) the ettringite-precipitation (volumetric variations above twice the initial volume) front. The dolomite-dissolution front, the smectite-dissolution front (volumetric variations below half of the initial volume) and the pH plume in the clay barrier (pH>9) were chosen to analyze clay-rock alterations. Dolomite is one of the most destabilized minerals in the claystone (Callovo–Oxfordian formation in this study) due to secondary phase formation (e.g., saponite) incorporating magnesium in their structural formulas, while montmorillonite (bearing hydroxyl groups) contributes to the buffer capacity. The criterion chosen for pH corresponds to a limit above which the dissolution rates of many aluminum silicate phases increase significantly. Regardless of the complexity of the simulation, after 100,000 years of interaction, not one of the above criteria indicates a perturbation higher than one meter. For the cases that account for full complexity, the perturbation extension is even 5 times lower. Still, in saturated conditions and besides the simulation conceptualization, the accuracy and numerical stability of the reactive transport codes have been successfully benchmarked (Blanc et al. 2015b). While simulations conducted in saturated conditions are numerous, simulations accounting for non-saturated and non-isothermal conditions are rare, making their results more difficult to evaluate. In these simulations, the main uncertainty lies in the period necessary to reach complete saturation inside the concrete. Considering an initial saturation of 30 %, this period is estimated to be approximately 2,000 years (Burnol et al. 2006), but it may depend on the grid size resolution and on the power exponent of the Millington relationship that describes dependency of pore aqueous and gas diffusion coefficients as a function of saturation and porosity (Trotignon et al. 2011). From the mineralogical point of view, the transformation pathways in concrete were found to be similar to those simulated in saturated conditions (e.g., portlandite degradation, carbonation, Ca to Si ratio decrease in C-S-H), except for sulfate/carbonate salts being deposited where drying takes place.

OTHER INTERFACES WITHOUT EXTENSIVE RTM STUDIES

The glass–(iron)–clay interface

This interface is studied in countries where the spent fuel is retreated, in total or in part, by removing and recycling uranium and plutonium, e.g., in Belgium, France, Germany, Japan, Russia, UK, and the USA (Gin et al. 2013). In this case, borosilicate glasses are developed as the waste matrix for HLLW. Note that preliminary studies have also been conducted for the use of glass for ILLW (e.g., in France, UK and the USA). This interface is complex, since iron may be present if steel corrosion is still going on when water enters the canister. Once corrosion is finished, corrosion products will be present and have an influence on glass alteration. RN can be considered as traces and are not thought to have a great impact on the glass alteration process.

Numerical studies of glass alteration at the space scale of the disposal cell (50 m) and the corresponding time scale (100,000 years) are scarce (Bildstein et al. 2007, 2012). In these simulations, glass alteration follows a very simple "operational" model in which the alteration proceeds in two stages, after a time lag corresponding to the time before canister failure (700 years): a first initial phase where the alteration rate (r_0) is high and a second stage where a residual, much lower, rate has been established (~r_0/10,000). The feedback between glass alteration and the chemical environment is indirectly taken into account by the duration of the initial stage, which stops when silica derived from the glass has saturated the "sorption" capacity of the system close to glass (essentially the corrosion products). In these simulations, iron corrosion starts at the beginning of the simulations so that from 700 to 45,000 years, when corrosion is completed, it proceeds simultaneously with glass alteration favoring the precipitation of Fe-silicates.

The most noticeable evolution in the RTM approach to glass alteration in these two studies concerns the complexity of the geochemical and mineral system. Bildstein et al. (2007) took into account only four simple mineral phases as glass alteration products, including one

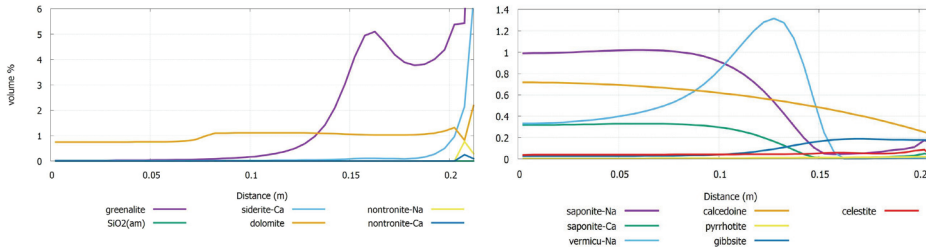

Figure 3. Profile of glass alteration products at 100,000 years in a 21 cm radius glass cylinder (Bildstein et al. 2012). Results obtained after alteration 5% of the initial volume of glass. Chalcedony, saponite, and vermiculite dominated in the center of the glass **(left plot)**. Greenalite and nontronite dominate towards the interface with iron, and Ca-siderite **(right plot)**.

zeolite. The second paper (Bildstein et al. 2012) includes 26 secondary minerals, with 14 glass alteration products, some of them determined from experimental studies (including Fe-silicates and Fe-aluminosilicates)(Figure 3). An explicit limitation of the H_2 partial pressure (hydrogen is considered to form a gas phase when pH_2 reaches 60 bar) was also taken into account as well as the presence of an excavation damaged zone with degraded transport properties in contact with the canister. Finally, to approach realistic conditions, the thermal gradient evolutions determined from THM calculations were included in the calculations, with temperature-dependent thermodynamic, kinetic and transport properties.

The relative simplicity of the simulations, in terms of glass behavior, can be explained by the fact that the alteration of glass in the presence of complex mineralogical environments has been only studied extensively in the last decade, allowing for specific models for glass alteration to be developed and calibrated.

Along with transport by diffusion, the dissolution of corrosion products and clay minerals and the precipitation of secondary crystallized minerals should be the main processes governing the long-term fate of glass. Dissolved cations such as Fe^{2+}, Mg^{2+}, Ni^{2+} have been shown to precipitate with silicon (if the pH is sufficiently high), which is the major element of the glass protective amorphous layer, and sustain glass dissolution (Aréna et al. 2016, 2017, 2018). The influence of Mg-rich Callovo–Oxfordian groundwater on glass dissolution has been modeled and fitted to the experimental results in Jollivet et al. (2012). The mechanism hypothesized by Rebiscoul et al. (2015) for modeling the long term alteration rate of glass in the presence of magnetite is slow magnetite dissolution followed by iron silicate precipitation. The ability of magnesium-rich minerals like hydromagnesite, dolomite and the argillite clay fraction to provide magnesium and sustain silicon consumption and glass alteration has been experimentally studied and modeled by (Debure et al. 2012, 2013, 2018). The effect of clay on glass alteration has often been described with a partition coefficient (Kd) of silicon in the clay, reflecting the complexity of the underlying dissolution/precipitation mechanisms (Godon et al. 1989; Gin et al. 2001; Pozo et al. 2007).

Current research in glass alteration modeling focuses on the description of the amorphous layer (formation, structure, composition, solubility) and on the capacity of the amorphous layer to lower the glass dissolution rate (Gin et al. 2016, 2018). Following an approach initiated by Bourcier et al. (1994), the hypothesis of a backward reaction of formation of the amorphous layer from the bulk fluid composition is made in order to build a thermodynamic description of the amorphous layer (McGrail and Chick 1984; Daux et al. 1997; Frugier et al. 2009; Rajmohan et al. 2010; Steefel et al. 2015a; Frugier and Godon 2018). The amorphous layer composition and solubility are currently described by concatenating database minerals or hypothetical phases that

account for both the amorphous layer composition and the fluid composition at steady state.The GRAAL model (Frugier 2008; Frugier and Godon 2018) computes the local amount of protective layer to calculate the local thickness of the protective layer and deduce the glass alteration rate.

The remaining challenge is to couple the specific model for glass alteration (e.g., GRAAL) with large-scale RTM simulations including the materials present in the near field of the disposal cell, i.e. to ensure compatibility between the two modeling systems.

The glass–concrete–(clay) interface

This interface plays a role in deep geological repository, especially in the Belgian concept of concrete supercontainer. Once the overpack (carbon steel) and primary container (stainless steel) have failed, glass will be in direct physical contact with concrete. There are currently no RTM studies of this interface at the scale of the disposal cell, to best of the authors' knowledge. This is partly due to the challenge of understanding the complex behavior of glass in water and its interactions with materials such as concrete, which has only been studied in recent years.

The glass–concrete interface has been a growing field of interest since Belgium proposed the supercontainer concept for the disposal of high-level wastes (Kursten and Druyts 2008). A thick concrete buffer is meant to maintain high pH, to preserve the integrity of the carbon steel overpack at least during the waste's thermal phase. France is studying the option of filling the gap between the rock wall and the casing with bentonite/cement grout. The grout thickness is dimensioned to compensate for acidic fluids coming from the oxidation of iron and sulfur in the clay occurring during the facility's operational period. With high pH for long periods of time, the Belgian concept relies more on the overpack's lifetime, whereas the French concept takes more advantage of the confinement properties of the waste glass. However, both require understanding, deterministic models, and long-term quantification relative to glass alteration close to concrete.

Alteration of glass at a pH higher than 10 results in the precipitation of other secondary crystallized minerals, especially zeolites, as well as C-S-H phases. Zeolite precipitation has been proven to sustain glass corrosion and to change the composition of the protective amorphous layer at the glass surface (Ribet and Gin 2004; Ferrand et al. 2013, 2014; Mercado-Depierre et al. 2013, 2017).

The higher the pH, the faster the zeolite nucleation-growth process and the slower the induction time required for zeolite surface to be high enough to impact the glass dissolution rate (Fournier et al. 2017). Zeolite precipitation consumes Si and Al, two key constituents in the amorphous layer, and therefore sustains glass dissolution. However, zeolites also consume alkali, which in return lowers both the pH and the zeolite precipitation rate. Zeolite-seeded experiments have been a major tool for investigating those experimental conditions where a mineral's precipitation kinetics drive the glass dissolution rate (Fournier et al. 2017). The first time-dependent geochemical modeling of alteration resumption has been achieved with the GRAAL model (Frugier et al. 2017). Only a limited number of modeling studies of glass–cement interactions exist and none of them integrated the transport component. Liu et al. (2015) report simulations of glass alteration in hyperalkaline solution from their 300-day experiments at the laboratory scale, showing a diffusion-controlled glass alteration rate at 30 °C and a shift towards a surface reaction-controlled rate after 100 days at 70 °C. Baston et al. (2017) performed batch type scoping thermodynamic modeling on the interactions between two illustrative vitrified ILLW products and two cementitious backfill, predicting limited changes in mineralogy and properties of the two materials. Improving knowledge about i) amorphous layer composition and solubility at high pH and ii) zeolite precipitation kinetics is still required before applying the model to the complex chemistry and the long time scales of geological disposal.

The iron–concrete interface in anoxic conditions

This interface will be encountered in the Belgian concept with the concrete supercontainers (steel envelope and overpack) and also in all type of repository concepts where steel reinforced concrete is envisaged. Although experimental studies on iron corrosion in concrete have been performed in the context of waste disposal (e.g., L'Hostis et al. 2011; Kursten et al. 2017), no RTM studies have been found in the literature concerning this interface in anoxic conditions.

In the highly alkaline interstitial solution of Portland concrete, the corrosion of carbon steel is characterized by a low corrosion rate (passive mode) in the order of 0.1 μm/yr to 1 μm/yr (Smart et al. 2013; Chomat et al. 2017; Kursten et al. 2017). This corrosion mode is due to the formation of a thin protective layer, with corrosion products similar to those observed at the iron–clay interface: magnetite dominates, accompanied by small amounts of hematite. The stability of this layer depends highly on the solution chemistry: pH, buffering effect, carbonate and sulfate content (Chomat et al. 2017). Corrosion can therefore resume when the conditions are no longer favorable, i.e. when concrete does not buffer the pH at high values (typically upon degradation by carbonation).

Since corrosion models are at the heart of this problematic, significant advances will be achieved in the near future by coupling RTM codes with electrochemical corrosion models (Bataillon et al. 2010; Macdonald et al. 2011).

GENERAL CONCLUSION AND PERSPECTIVES

Over the last two decades, the use of RTM in simulations of the long-term behavior of materials in waste repositories has evolved to consider geochemical systems of increasing complexity, driven by the improvement of numerical codes (more functionalities), and their efficiency (solver, parallelization), as well as the accumulation of data acquired to feed thermodynamic and kinetics databases. Overall, these simulations provide a better understanding of physical and chemical change and how materials interact; they give more confidence in the prediction of the durability of materials by converging on the alteration extent that can be expected at the interfaces between different materials over long periods of time. Benchmarking RTM codes on problems related to waste repositories (e.g., Marty et al. 2015b) and continuous database development (Blanc et al. 2012, 2015b; Giffaut et al. 2014; Lothenbach et al. 2019) also improve the robustness of the predictions. This is not to say that we fully understand all the physical and chemical phenomena or that modeling is fully representative of all the processes occurring in such complex systems. These are two different aspects to be considered which call for different treatment: either acquiring more scientific knowledge through experiments, or new developments or approaches in numerical codes. Often, both issues have to be tackled together.

An example of the "lack of knowledge" issue is the question of how redox conditions are controlled in deep geological environments (e.g., see the results of redox measurements in European project RECOSY (Duro et al. 2014). Oxygen is a very reactive chemical compound, readily producing oxic conditions along its diffusive pathway during the operational stage (see dedicated section in this chapter). These oxic conditions will not remain long after the closure of the disposal cells and the onset of the corrosion phase. The re-establishment of reduced conditions in the host rock is expected within a few hundreds to thousands of years. Moreover, reduced conditions do not mean reducing conditions, i.e. the formation of reactive reductants: the reactivity of hydrogen is low, sulfate reduction is thought to be very slow and only catalyzed by microorganisms (Truche et al. 2009) and argillaceous rocks only contain small amounts of ferric compounds (e.g., in the Callovo–Oxfordian claystone). The question therefore remains about the buffering capacity of the host rock with respect to additional

oxidative perturbations once the hydrogen has diffused away from the cell disposal. Such perturbations could come from the alteration of glass that will release significant amounts of ferric species. This is of course a crucial issue for the concomitant migration of RNs. It is not clear whether the host rock will contain enough reactive reductants (ferrous and/or sulfide compounds, such as pyrite) to maintain reduced conditions at this stage. Most RTM codes are ready to simulate this type of situation, since redox couples can usually be deactivated to define only the reactive ones (even H^+/H_2 in post-corrosion conditions).

Another recurrent issue in RTM is the value of reactive surface area that should be used for minerals in the simulation of these systems (see discussion in Li 2019, this volume). An example of assessment of the reactive surface of glass dissolving in water is given by Fournier et al. (2016), who demonstrated that the use of geometrical surface area provides a consistent approach whenever it can be easily calculated. When trying to apply this approach to porous media, and even more so to evolving porous media, the question is inevitably linked to the concepts of porosity network, accessibility to water, and physical and chemical heterogeneities (e.g., Landrot et al. 2012, Noiriel et al. 2012). Variable porosity is the result of the volume balance between mineral dissolution and precipitation (Seigneur et al. 2019, this volume); clogging phenomena are predicted at the interfaces between reactive materials in the repository because secondary minerals take up more volume than primary minerals. This is particularly true for metallic components, especially if technological gaps are rapidly filled by swelling clay upon rehydration (Wilson et al. 2015). This behavior is also predicted at the interface between concrete and clay. No consensus has been reached today about how the RT processes are affected by porosity clogging, i.e. how the macroscopic mineral reaction rate changes when porosity vanishes. This is a domain where RT simulations at the pore scale could help decipher the mechanisms controlling the dissolution and precipitation rate (Molins and Knabner 2019, this volume). A corollary aspect of this question brings us to the way we consider the evolution of transport properties in (strongly) altered zones. For instance, the diffusion properties in the corrosion layer, which controls the mineral sequence of corrosion products, had to be set to very low values to reproduce the observed paragenesis (Bildstein et al. 2016). In these situations, Kozeny–Carman and Archie's law fail to reproduce experimental observations and thermodynamic properties such as solubility are also modified if pores reach micrometric size (e.g. Emmanuel and Berkowitz 2007, Mürmann et al. 2013, Bergonzi et al. 2016, Rajyaguru et al. 2019). Although the precipitation of minerals, in general and in particular in this type of pores, should theoretically be described in RTM as a sequence of steps including nucleation, scavenging (or ripening), and growth, this approach has only been used by Savage et al. (2010) in the context of waste repositories. This type of model has been developed in the last decade and could be used more widely, providing that the necessary data are acquired (Fritz and Noguera 2009, Noguera et al. 2006, 2016). Combined with the thermodynamic approach in small pores, they may also shed new light on the processes controlling mineral reactivity during porosity clogging.

Recognizing that the combination of heat release in HLLW disposal cells and the production of hydrogen gas (also in the ILLW cells) will significantly delay the resaturation of the repository near field, more THC processes have been implemented to perform simulations with realistic temperature and water saturation changes during the lifetime of the repository. Multiphase RTM has been conducted, first looking at TH processes with a source of hydrogen (e.g., Xu et al. 2008, Zheng et al. 2008, Senger et al. 2011, Treille et al. 2012). It has progressively integrated more complex chemistry (e.g., pyrite oxidation in De Windt et al. 2014; bentonite illitization in Zheng et al. 2015), but full chemical treatment has been limited so far mainly to concrete carbonation (Trotignon et al. 2011, Thouvenot et al. 2013). The coupling between the fast diffusive transport of very reactive gas has proven to be a challenge for numerical codes. In this regard, the RTM of waste repositories could benefit from the experience return of modeling in other systems such as CO_2 sequestration (Sin and Corvisier 2019, this volume). Another aspect of unsaturated porous media that is not yet widely treated

in RTM relates to the dependence of chemical reactivity with regard to the water content, in particular looking at how the mineral and gas solubility and the aqueous speciation relate to capillary pressure at low water saturation (Lassin et al. 2005, 2011, 2016). This process may be enhanced by the fact that some chemical reactions, such as steel corrosion and glass alteration, consume water; this coupled effect is only starting to be fully integrated in RTM codes (Seigneur et al. 2018).

Finally, even though large-scale 3D RTM calculations started to be tractable very recently thanks to improvements in computer calculation capacity, studies looking at waste repositories in this way are scarce (Trinchero et al. 2017). The main reason remains the large scale of the problems considered: metric to kilometric spatial domain, time period of 100,000 to millions of years. This explains, at least partly, why numerical simulations in this context have not yet fully benefited from recent advancements in RTM such as the diffusion in charged porous media (Tournassat and Steefel 2019, this volume). This feature would be particularly appropriate for clay materials encountered in deep geological storage to account for different "porosities" accessible to anions and cations. The same statement is applicable for modeling at the pore scale, which could be combined with the macroscopic approach, for instance, for problems involving porosity clogging.

REFERENCES

Alexander WR, Dayal R, Eagleson K, Eikenberg J, Hamilton E, Linklater CM, McKinley IG, Tweed CJ (1992) A natural analogue of high pH cement pore waters from the Maqarin area of northern Jordan. II: Results of predictive geochemical calculations. J Geochem Explor 46:133–146

Alexander WR, Reijonen HM, McKinley IG (2015) Natural analogues: studies of geological processes relevant to radioactive waste disposal in deep geological repositories. Swiss J Geosci 108:75–100

Alonso MC, García Calvo JL, Hidalgo A, Fernández Luco L (2010) Development and application of low-pH concretes for structural purposes in geological repository systems. *In:* Geological Repository Systems for Safe Disposal of Spent Nuclear Fuels and Radioactive Waste. Ahn J, Apted MJ, (eds). Woodhead Publishing, p 286–322

Altmann S, Tournassat C, Goutelard F, Parneix JC, Gimmi T, Maes N (2012) Diffusion-driven transport in clayrock formations. Appl Geochem 27:463–478

Andra (2005) Dossier 2005: Argile Synthesis. Evaluation of the Feasibility of a Geological Repository in an Argillaceous Formation Meuse/Haute-Marne Site. National Agency for Radioactive Waste Management, Paris.

Andra (2009) JALON 2009 HA-MAVL - Options de conception du stockage en formation géologique profonde. Report C.NSY.ASTE.08.0429.A, National Agency for Radioactive Waste Management, Paris

Apted M, Ahn J (2010) Multiple-barrier geological repository design and operation strategies for safe disposal of radioactive materials. *In:* Geological Repository Systems for Safe Disposal of Spent Nuclear Fuels and Radioactive Waste. Ahn J, Apted MJ, (eds). Woodhead Publishing, p 3–28

Arcos D, Bruno J, Karnland O (2003) Geochemical model of the granite–bentonite–groundwater interaction at Äspö HRL (LOT experiment). Appl Clay Sci 23:219–228

Arcos D, Grandia F, Domènech C, Fernandez AM, Villar MV, Muurinen A, Carlsson T, Sellin P, Hernan P (2008) Long-term geochemical evolution of the near field repository: Insights from reactive transport modelling and experimental evidences. J Contam Hydrol 102:196–209

Aréna H, Godon N, Rebiscoul D, Podor R, Garces E, Cabie M, Mestre JP (2016) Impact of Zn, Mg, Ni and Co elements on glass alteration: Additive effects. J Nucl Mater 470:55–67

Aréna H, Godon N, Rébiscoul D, Frugier P, Podor R, Garcès E, Cabie M, Mestre JP (2017) Impact of iron and magnesium on glass alteration: Characterization of the secondary phases and determination of their solubility constants. Appl Geochem 82:119–133

Aréna H, Rébiscoul D, Podor R, Garcès E, Cabie M, Mestre JP, Godon N (2018) Impact of Fe, Mg and Ca elements on glass alteration: Interconnected processes. Geochim Cosmochim Acta 239:420–445

Armand G, Leveau F, Nussbaum C, de La Vaissiere R, Noiret A, Jaeggi D, Landrein P, Righini C (2014) Geometry and Properties of the Excavation-Induced Fractures at the Meuse/Haute-Marne URL Drifts. Rock Mech Rock Eng 47:21–41

Ashraf W (2016) Carbonation of cement-based materials: Challenges and opportunities. Constr Build Mater 120:558–570

Audoly R, Vogt-Schilb A, Guivarch C, Pfeiffer A (2018) Pathways toward zero-carbon electricity required for climate stabilization. Appl Energy 225:884–901

Auroy M, Poyet S, Le Bescop P, Torrenti JM (2013) Impact of carbonation on the durability of cementitious materials: water transport properties characterization. EPJ Web of Conferences 56 01008

Auroy M, Poyet S, Le Bescop P, Torrenti J-M, Charpentier T, Moskura M, Bourbon X (2015) Impact of carbonation on unsaturated water transport properties of cement-based materials. Cem Concr Res74:44–58

Auroy M, Poyet Sp, Le Bescop P, Torrenti J-M, Charpentier T, Moskura Ml, Bourbon X (2018) Comparison between natural and accelerated carbonation (3% CO_2): Impact on mineralogy, microstructure, water retention and cracking. Cem Concr Res 109:64–80

Avis J, Suckling P, Calder N, Walsh R, Humphreys P, King F (2013) T2GGM: A coupled gas generation model for deep geologic disposal of radioactive waste. Nucl Technol 187:175–187

Bach TTH, Coumes CCD, Pochard I, Mercier C, Revel B, Nonat A (2012) Influence of temperature on the hydration products of low pH cements. Cem Concr Res 42:805–817

Bamforth P, Baston G, Berry J, Glasser F, Heath T, Jackson C, Savage D, Sawanton S (2012) Cement materials for use as backfill, sealing and structural materials in geological disposal concepts. Report SERCO/005125/001, Serco, Harwell, Oxfordshire

Barnichon JD, Dauzeres A, De Windt L (2018) Understanding oxidizing transient conditions in clayey rocks. Appl Geochem 98:435–447

Bartier D, Techer I, Dauzères A, Boulvais P, Blanc-Valleron M-M, Cabrera J (2013) In situ investigations and reactive transport modelling of cement paste/argillite interactions in a saturated context and outside an excavated disturbed zone. Appl Geochem 31:94–108

Bary B, Mügler C (2006) Simplified modelling and numerical simulations of concrete carbonation in unsaturated conditions. Revue Européenne Génie Civil 10:1049–1072

Bary B, Sellier A (2004) Coupled moisture-carbon dioxide-calcium transfer model for carbonation of concrete. Cem Concr Res 34:1859–1872

Baston G, Heath T, Hunter F, Swanton S (2017) Modelling of cementitious backfill interactions with vitrified intermediate-level waste. Phys Chem Earth, Parts A/B/C 99:121–130

Bataillon C, Bouchon F, Chainais-Hillairet C, Desgranges C, Hoarau E, Martin F, Perrin S, Tupin M, Talandier J (2010) Corrosion modelling of iron based alloy in nuclear waste repository. Electrochim Acta 55:4451–4467

Benbow S, Wilson J, Metcalfe R, Lehikoinen J (2019) Avoiding unrealistic behaviour in coupled reactive-transport simulations of cation exchange and mineral kinetics in clays. Clay Minerals:1–11

Benet L-V, Bouillet C, Wendling J (2014a) Analysis of the ambient conditions in an IL-LLW storage cell in a deep clay repository during the waiting closure period. *In:* Clays in Natural and Engineered Barriers for Radioactive Waste Confinement. Vol 400. Norris S, Bruno J, Cathelineau M, Delage P, Fairhurst C, Gaucher EC, Hohn EH, Kalinichev A, Lalieux P, Sellin P, (eds). p 145–161

Benet L-V, Tulita C, Calsyn L, Wendling J (2014b) Evolution of temperature and humidity in an underground repository over the operation period. *In:* Clays in Natural and Engineered Barriers for Radioactive Waste Confinement. Vol 400. Norris S, Bruno J, Cathelineau M, Delage P, Fairhurst C, Gaucher EC, Hohn EH, Kalinichev A, Lalieux P, Sellin P, (eds). Geol Soc Spec Publ, p 413–426

Bergonzi I, Mercury L, Simon P, Jamme F, Shmulovich K (2016) Oversolubility in the microvicinity of solidâ€“solution interfaces. Phys Chem Chem Phys 18:14874–14885

Berner U, Kulik DA, Kosakowski G (2013) Geochemical impact of a low-pH cement liner on the near field of a repository for spent fuel and high-level radioactive waste. Phys Chem Earth, Parts A/B/C 64:46–56

Bernier F, Lemy F, De Cannière P, Detilleux V (2017) Implications of safety requirements for the treatment of THMC processes in geological disposal systems for radioactive waste. J Rock Mech Geotech Eng 9:428–434

Bildstein O, Claret F (2015) Chapter 5—Stability of Clay Barriers Under Chemical Perturbations. *In:* Developments in Clay Science. Vol Volume 6. Tournassat C, Steefel CI, Bourg IC, Faiza B, (eds). Elsevier, p 155–188

Bildstein O, Trotignon L, Perronnet M, Jullien M (2006) Modelling iron–clay interactions in deep geological disposal conditions. Phys Chem Earth, Parts A/B/C 31:618–625

Bildstein O, Trotignon L, Pozo C, Jullien M (2007) Modelling glass alteration in an altered argillaceous environment. J Nucl Mater 362:493–501

Bildstein O, Lartigue J, Pointeau I, Cochepin B, Munier I, Michau N (2012) Chemical evolution in the near field of HLW cells: interactions between glass, steel and clay-stone in deep geological conditions. 5th ANDRA International Meeting, 22–25 Oct 2012, Montpellier, France

Bildstein O, Lartigue J-E, Schlegel ML, Bataillon C, Cochepin Bt, Munier I, Michau N (2016) Gaining insight into corrosion processes from numerical simulations of an integrated iron-claystone experiment. Geol Soc, London, Spec Publ 443:253–267

Blanc P, Bourbon X, Lassin A, Gaucher EC (2010) Chemical model for cement-based materials: Temperature dependence of thermodynamic functions for nanocrystalline and crystalline C-S-H phases. Cem Concr Res 40:851–866

Blanc P, Lassin A, Piantone P, Azaroual M, Jacquemet N, Fabbri A, Gaucher EC (2012) Thermoddem: A geochemical database focused on low temperature water/rock interactions and waste materials. Appl Geochem 27:2107–2116

Blanc P, Vieillard P, Gailhanou H, Gaboreau S, Gaucher E, Fialips CI, Made B, Giffaut E (2015a) A generalized model for predicting the thermodynamic properties of clay minerals. American Journal of Science 315:734–780

Blanc P, Vieillard P, Gailhanou H, Gaboreau S, Marty N, Claret F, Madé B, Giffaut E (2015b) ThermoChimie database developments in the framework of cement/clay interactions. Appl Geochem 55:95–107

Bond A, Benbow S, Wilson J, Millard A, Nakama S, English M, McDermott C, Garitte B (2013) Reactive and non-reactive transport modelling in partially water saturated argillaceous porous media around the ventilation experiment, Mont Terri. J Rock Mech Geotech Eng 5:44–57

Bourcier WL, Carroll SA, Phillips BL (1994) Constraints on the affinity term for modeling long-term glass dissolution rates. *In:* Scientific Basis for Nuclear Waste Management XVII. Vol 333. Barkatt A, Van Konynenburg RA, (eds). Mater. Res. Soc., Pittsburgh, PA, p 507–512

Bourdelle F, Truche L, Pignatelli I, Mosser-Ruck R, Lorgeoux C, Roszypal C, Michau N (2014) Iron–clay interactions under hydrothermal conditions: Impact of specific surface area of metallic iron on reaction pathway. Chem Geol 381:194–205

Bourdelle F, Mosser-Ruck R, Truche L, Lorgeoux C, Pignatelli I, Michau N (2017) A new view on iron-claystone interactions under hydrothermal conditions (90 °C) by monitoring in situ pH evolution and H_2 generation. Chem Geol 466:600–607

Bradbury MH, Baeyens B (2003) Porewater chemistry in compacted re-saturated MX-80 bentonite. J Contam Hydrol 61:329–338

Bradbury MH, Baeyens B (2009) Experimental and modelling studies on the pH buffering of MX-80 bentonite porewater. Appl Geochem 24:419–425

Brantley SL, Holleran ME, Jin L, Bazilevskaya E (2013) Probing deep weathering in the Shale Hills Critical Zone Observatory, Pennsylvania (USA): the hypothesis of nested chemical reaction fronts in the subsurface. Earth Surface Processes and Landforms 38:1280–1298

Bredehoeft JD (2003) From models to performance assessment: the conceptualization problem. Groundwater 41:571–577

Brendler V, Vahle A, Arnold T, Bernhard G, Fanghänel T (2003) RES3T-Rossendorf expert system for surface and sorption thermodynamics. J Contam Hydrol 61:281–291

Brommundt J, Kaempfer TU, Enssle CP, Mayer G, Wendling J (2014) Full-scale 3D modelling of a nuclear waste repository in the Callovo–Oxfordian clay. Part 1: thermo-hydraulic two-phase transport of water and hydrogen. Geological Society, London, Special Publications 400:SP400.434

Brook BW, Alonso A, Meneley DA, Misak J, Blees T, van Erp JB (2014) Why nuclear energy is sustainable and has to be part of the energy mix. Sustainable Mater Technol 1–2:8–16

Burkan Isgor O, Razaqpur AG (2004) Finite element modeling of coupled heat transfer, moisture transport and carbonation processes in concrete structures. Cement and Concrete Composites 26:57–73

Burnol A, Blanc P, Xu T, Spycher N, Gaucher EC (2006) Uncertainty in the reactive transport model response to an alkaline perturbation in a clay formation. TOUGH Symposium 2006, Berkeley, California

Chaou A, Abdelouas A, Mendilia YE, Martin C (2017) The role of pH in the vapor hydration at 175 °C of the French SON68 glass. Appl Geochem 76:22–35

Chaparro MC, Saaltink MW, Soler JM (2017) Reactive transport modelling of cement-groundwater–rock interaction at the Grimsel Test Site. Phys Chem Earth 99:64–76

Chapman N, Hooper A (2012) The disposal of radioactive wastes underground. Proc Geol Assoc 123:46–63

Chomat L, Amblard E, Varlet J, Blanc C, Bourbon X (2017) Passive corrosion of steel reinforcement in blended cement-based material in the context of nuclear waste disposal. Corrosion Eng Sci Technol 52:148–154

Cici G, Cembalo L, Del Giudice T, Palladino A (2012) Fossil energy versus nuclear, wind, solar and agricultural biomass: Insights from an Italian national survey. Energy Policy 42:59–66

Claret F, Sakharov BA, Drits VA, Velde B, Meunier A, Griffault L, Lanson B (2004) Clay minerals in the Meuse-Haute marne underground laboratory (France): Possible influence of organic matter on clay mineral evolution. Clays Clay Minerals 52:515–532

Claret F, Marty N, Tournassat C (2018a) Modeling the long-term stability of multi-barrier systems for nuclear waste disposal in geological clay formations. *In:* Reactive Transport Modeling: Applications in Subsurface Energy and Environmental Problems. Yitian X, Fiona W, Tianfu X, Carl S, (eds). John Wiley & Sons Ltd., 395–451

Claret F, Grangeon S, Loschetter A, Tournassat C, De Nolf W, Harker N, Boulahya F, Gaboreau S, Linard Y, Bourbon X, Fernandez-Martinez A (2018b) Deciphering mineralogical changes and carbonation development during hydration and ageing of a consolidated ternary blended cement paste. IUCrJ 5:150–157

Codina M, Cau-dit-Coumes C, Le Bescop P, Verdier J, Ollivier JP (2008) Design and characterization of low-heat and low-alkalinity cements. Cem Concr Res38:437–448

Craen MD, Geet MV, Honty M, Weetjens E, Sillen X (2008) Extent of oxidation in Boom Clay as a result of excavation and ventilation of the HADES URF: Experimental and modelling assessments. Phys Chem Earth, Parts A/B/C 33, Supplement 1:S350-S362

Cronstrand P (2014) Evolution of pH in SFR 1. SKB report TR-14–01, Swedish Nuclear Fuel and Waste Management Company, Stockholm, Sweden

Czarnecki L, Woyciechowski P (2015) Modelling of concrete carbonation; is it a process unlimited in time and restricted in space? Bull Polish Acad Sci Tech Sci 63:43–54

Daux V, Guy C, Advocat T, Crovisier JL, Stille P (1997) Kinetic aspects of basaltic glass dissolution at 90 °C : role of aqueous silicon and aluminium. Chem Geol 142:109–126

Dauzeres A, Achiedo G, Nied D, Bernard E, Alahrache S, Lothenbach B (2016) Magnesium perturbation in low-pH concretes placed in clayey environment-solid characterizations and modeling. Cem Concr Res 79:137–150

de Combarieu G, Barboux P, Minet Y (2007) Iron corrosion in Callovo–Oxfordian argilite: From experiments to thermodynamic/kinetic modelling. Phys Chem Earth, Parts A/B/C 32:346–358

De Marsily G, Ledoux E, Barbreau A, Margat J (1977) Nuclear Waste Disposal: Can the Geologist Guarantee Isolation? Science 197:519–527
De Windt L, Pellegrini D, van der Lee J (2004) Coupled modeling of cement/claystone interactions and radionuclide migration. J Contam Hydrol 68:165–182
De Windt L, Marsal F, Tinseau E, Pellegrini D (2008) Reactive transport modeling of geochemical interactions at a concrete/argillite interface, Tournemire site (France). Phys Chem Earth 33:S295-S305
De Windt L, Marsal F, Corvisier J, Pellegrini D (2014) Modeling of oxygen gas diffusion and consumption during the oxic transient in a disposal cell of radioactive waste. Appl Geochem 41:115–127
De Windt L, Bertron A, Larreur-Cayol S, Escadeillas G (2015) Interactions between hydrated cement paste and organic acids: Thermodynamic data and speciation modeling. Cem Concr Res69:25–36
Debure M, Frugier P, De Windt L, Gin S (2012) Borosilicate glass alteration driven by magnesium carbonates. J Nucl Mater 420:347–361
Debure M, Frugier P, De Windt L, Gin S (2013) Dolomite effect on borosilicate glass alteration. Appl Geochem 33:237–251
Debure M, De Windt L, Frugier P, Gin S (2018) Mechanisms involved in the increase of borosilicate glass alteration by interaction with the Callovian-Oxfordian clayey fraction. Appl Geochem 98:206–220
Dillmann P, Neff D, Féron D (2014) Archaeological analogues and corrosion prediction: from past to future. A review. Corros Eng Sci Technol 49:567–576
Drouet E (2010) Impact de la température sur la carbonatation des matériaux cimentaires—prise en compte des transferts hydriques, Thèse de Doctorat. ENS Cachan.
Drouet E, Poyet Sp, Le Bescop P, Torrenti J-M, Bourbon X (2018) Carbonation of hardened cement pastes: Influence of temperature. Cem Concr Res115:445–459
Duro L, Bruno J, Grivé M, Montoya V, Kienzler B, Altmaier M, Buckau G (2014) Redox processes in the safety case of deep geological repositories of radioactive wastes. Contribution of the European RECOSY Collaborative Project. Appl Geochem 49:206–217
El Hajj H, Abdelouas A, El Mendili Y, Karakurt G, Grambow B, Martin C (2013) Corrosion of carbon steel under sequential aerobic-anaerobic environmental conditions. Corros Sci 76:432–440
Emmanuel S, Berkowitz B (2007) Effects of pore-size controlled solubility on reactive transport in heterogeneous rock. Geophys Res Lett 34: L06404
Enssle CP, Brommundt J, Kaempfer TU, Mayer G, Wendling J (2014) Full-scale 3D modelling of a nuclear waste repository in the Callovo–Oxfordian clay. Part 2: thermo-hydraulic two-phase transport of water, hydrogen, ^{14}C and ^{129}I. Geol Soc, London, Spec Publ 400:469–481
Ewing RC (2015) Long-term storage of spent nuclear fuel. Nat Mater 14:252
Fernandez R, Cuevas J, Mader UK (2010) Modeling experimental results of diffusion of alkaline solutions through a compacted bentonite barrier. Cem Concr Res 40:1255–1264
Féron D, Crusset D, Gras J-M (2008) Corrosion issues in nuclear waste disposal. J Nucl Mater379:16–23
Ferrand K, Lui S, Lemmens K (2013) The interaction between nuclear waste glass dans ordinary Portand cement. Int J Appl Glass Sci 4:328–340
Ferrand K, Liu S, Lemmens K (2014) The effect of ordinary portland cement on nuclear waste glass dissolution. Procedia Mater Sci 7:223–229
Fournier M, Ull A, Nicoleau E, Inagaki Y, Odorico M, Frugier P, Gin S (2016) Glass dissolution rate measurement and calculation revisited. J Nucl Mater 476:140–154
Fournier M, Gin S, Frugier P, Mercado-Depierre S (2017) Contribution of zeolite-seeded experiments to the understanding of resumption of glass alteration. Mater Degradation 1:17
Fritz B, Noguera C (2009) Mineral precipitation kinetics. Rev Mineral Geochem 70:371–410
Frugier P, Godon N (2018) Effet de la stœchiométrie Si-Mg des produits d'altération sur la modélisation GRAAL. CEA report DTCD/SEVT/2018–20, 31 p.
Frugier P, Gin S, Minet Y, Chave T, Bonin B, Godon N, Lartigue JE, Jollivet P, Ayral A, De Windt L, Santarini G (2008) SON68 Nuclear glass dissolution kinetics: Current state of knowledge and basis of the new GRAAL model. J Nucl Mater 380:8–21
Frugier P, Chave T, Gin S, Lartigue JE (2009) Application of the GRAAL model to leaching experiments with SON68 nuclear glass in initially pure water. J Nucl Mater 392:552–567
Frugier P, Fournier M, Gin S (2017) Modeling resumption of glass alteration due to zeolites precipitation. Procedia Earth Planet Sci 17:340–343
Gaboreau S, Prêt D, Tinseau E, Claret F, Pellegrini D, Stammose D (2011) 15 years of in situ cement–argillite interaction from Tournemire URL: Characterisation of the multi-scale spatial heterogeneities of pore space evolution. Appl Geochem 26:2159–2171
Gaboreau S, Prêt D, Montouillout V, Henocq P, Robinet J-C, Tournassat C (2017) Quantitative mineralogical mapping of hydrated low pH concrete. Cem Concr Compos 83:360–373
Gailhanou H, van Miltenburg JC, Rogez J, Olives J, Amouric M, Gaucher EC, Blanc P (2007) Thermodynamic properties of anhydrous smectite MX-80, illite IMt-2 and mixed-layer illite-smectite ISCz-1 as determined by calorimetric methods. Part I: Heat capacities, heat contents and entropies. Geochim Cosmochim Acta 71:5463–5473

Gailhanou H, Rogez J, van Miltenburg JC, van Genderen ACG, Greneche JM, Gilles C, Jalabert D, Michau N, Gaucher EC, Blanc P (2009) Thermodynamic properties of chlorite CCa-2. Heat capacities, heat contents and entropies. Geochim Cosmochim Acta 73:4738–4749

Gailhanou H, Blanc P, Rogez J, Mikaelian G, Kawaji H, Olives J, Amouric M, Denoyel R, Bourrelly S, Montouillout V, Vieillard P (2012) Thermodynamic properties of illite, smectite and beidellite by calorimetric methods: Enthalpies of formation, heat capacities, entropies and Gibbs free energies of formation. Geochim Cosmochim Acta 89:279–301

Gailhanou H, Blanc P, Rogez J, Mikaelian G, Horiuchi K, Yamamura Y, Saito K, Kawaji H, Warmont F, Grenèche JM, Vieillard P (2013) Thermodynamic properties of saponite, nontronite, and vermiculite derived from calorimetric measurements. Am Mineral 98:1834–1847

Gailhanou H, Vieillard P, Blanc P, Lassin A, Denoyel R, Bloch E, De Weireld G, Gaboreau S, Fialips CI, Madé B, Giffaut E (2017) Methodology for determining the thermodynamic properties of smectite hydration. Appl Geochem 82:146–163

García Calvo JL, Hidalgo A, Alonso C, Fernández Luco L (2010) Development of low-pH cementitious materials for HLRW repositories: Resistance against ground waters aggression. Cem Concr Res 40:1290–1297

Gaucher EC, Blanc P (2006) Cement/clay interactions—A review: Experiments, natural analogues, and modeling. Waste Manage 26:776–788

Gaucher E, Robelin C, Matray JM, Negral G, Gros Y, Heitz JF, Vinsot A, Rebours H, Cassagnabere A, Bouchet A (2004a) ANDRA underground research laboratory: interpretation of the mineralogical and geochemical data acquired in the Callovian-Oxfordian formation by investigative drilling. Phys Chem Earth 29:55–77

Gaucher EC, Blanc P, Matray JM, Michau N (2004b) Modeling diffusion of an alkaline plume in a clay barrier. Appl Geochem 19:1505–1515

Geckeis H, Rabung T (2008) Actinide geochemistry: From the molecular level to the real system. J Contam Hydrol 102:187–195

Giffaut E, Grivé M, Blanc P, Vieillard P, Colàs E, Gailhanou H, Gaboreau S, Marty N, Madé B, Duro L (2014) Andra thermodynamic database for performance assessment: ThermoChimie. Appl Geochem 49:225–236

Gin S, Jollivet P, Mestre J, Jullien M, Pozo C (2001) French SON 68 nuclear glass alteration mechanisms on contact with clay media. Appl Geochem 16:861–881

Gin S, Abdelouas A, Criscenti LJ, Ebert WL, Ferrand K, Geisler T, Harrison MT, Inagaki Y, Mitsui S, Mueller KT, Marra JC (2013) An international initiative on long-term behavior of high-level nuclear waste glass. Mater Today 16:243–248

Gin S, Jollivet P, Fournier M, Angeli F, Frugier P, Charpentier T (2015) Origin and consequences of silicate glass passivation by surface layers. Nat Commun 6:6360

Gin S, Neill L, Fournier M, Frugier P, Ducasse T, Tribet M, Abdelouas A, Parruzot B, Neeway J, Wall N (2016) The controversial role of inter-diffusion in glass alteration. Chem Geol 440:115–123

Gin S, Collin M, Jollivet P, Fournier M, Minet Y, Dupuy L, Mahadevan T, Kerisit S, Du J (2018) Dynamics of self-reorganization explains passivation of silicate glasses. Nat Commun 9:2169

Glassley WE, Nitao JJ, Grant CW (2003) Three-dimensional spatial variability of chemical properties around a monitored waste emplacement tunnel. J Contam Hydrol 62–63:495–507

Godon N, Vernaz E, Thomassin JH, Touray JC (1989) Effect of environmental materials on aqueous corrosion of R7T7 glass. *In:* Scientific Basis for Nuclear Waste Management XII. Vol 127. Werner L, (ed) Mater Res Soc, Pittsburgh, PA, p 97–104

Gong WL, Lutze W, Abdelouas A, Ewing RC (1999) Vitrification of radioactive waste by reaction sintering under pressure. J Nucl Mater 265:12–21

Grambow B (2008) Mobile fission and activation products in nuclear waste disposal. J Contam Hydrol 102:180–186

Grambow B, Bretesché S (2014) Geological disposal of nuclear waste: II. From laboratory data to the safety analysis—Addressing societal concerns. Appl Geochem 49:247–258

Grenthe I (1991) Thermodynamics in migration chemistry. Radiochimica Acta 52–53:425–432

Groves GW, Rodway DI, Richardson IG (1990) The carbonation of hardened cement pastes. Adv Cem Res 3:117–125

Hess HH (1957) The Disposal of Radioactive Waste on Land: Report of the Committee on Waste Disponal of the Division of Earthsciences [chairman Harry H. Hess]. National Academy of Sciences, National Research Council

Hoch A, Wendling J (2011) Migration of gases around a cell containing high-activity vitrified wastes during the operational phase. Phys Chem Earth, Parts A/B/C 36:1743–1753

Hoerlé S, Mazaudier F, Dillmann P, Santarini G (2004) Advances in understanding atmospheric corrosion of iron. II. Mechanistic modelling of wet–dry cycles. Corros Sci 46:1431–1465

Höglund L (2001) Modelling of long-term concrete degradation processes in the Swedish SFR repository. SKB report TR-01–08, Swedish Nuclear Fuel and Waste Management Company, Stockholm, Sweden

Höglund L (2013) The impact of concrete degradation on the BMA barrier functions. SKB report TR-13–40, Swedish Nuclear Fuel and Waste Management Company, Stockholm, Sweden

Huang Y, Shao H, Wieland E, Kolditz O, Kosakowski G (2018) A new approach to coupled two-phase reactive transport simulation for long-term degradation of concrete. Constr Build Mater 190:805–829

Hummel W, Schneider JW (2005) Safety of nuclear waste repositories. Chimia 59:909–915

Hummel W, Berner U, Curti E, Pearson F, Thoenen T (2002) Nagra/PSI chemical thermodynamic data base 01/01. Radiochim Acta 90:805–813
Hunter F, Bate F, Heath T, Hoch A (2007) Geochemical investigation of iron transport into bentonite as steel corrodes. SKB report TR-07–09
Jenni A, Mäder U, Lerouge C, Gaboreau S, Schwyn B (2014) In situ interaction between different concretes and Opalinus Clay. Phys Chem Earth, Parts A/B/C
Jenni A, Gimmi T, Alt-Epping P, Mader U, Cloet V (2017) Interaction of ordinary Portland cement and Opalinus Clay: Dual porosity modelling compared to experimental data. Phys Chem Earth 99:22–37
Johnson L, King F (2008) The effect of the evolution of environmental conditions on the corrosion evolutionary path in a repository for spent fuel and high-level waste in Opalinus Clay. J Nucl Mater 379:9–15
Johnson B, Newman A, King J (2017) Optimizing high-level nuclear waste disposal within a deep geologic repository. Ann Oper Res 253:733–755
Jollivet P, Frugier P, Parisot G, Mestre JP, Brackx E, Gin S (2012) Effect of clayey groundwater on the dissolution rate of the simulated nuclear waste glass SON68. J Nucl Mater 420:508–518
Khoury HN, Salameh E, Abdul-Jaber Q (1985) Characteristics of an unusual highly alkaline water from the Maqarin area, northern Jordan. J Hydrol 81:79–91
Khoury HN, Salameh E, Clark ID, Fritz P, Bajjali W, Milodowski AE, Cave MR, Alexander WR (1992) A natural analogue of high pH cement pore waters from the Maqarin area of northern Jordan. I: introduction to the site. J Geochem Explor 46:117–132
King F (2014) Predicting the lifetimes of nuclear waste containers. JOM 66:526–537
King F, Shoesmith DW (2010) 13 - Nuclear waste canister materials, corrosion behaviour and long-term performance in geological repository systems. *In:* Geological Repository Systems for Safe Disposal of Spent Nuclear Fuels and Radioactive Waste. Ahn J, Apted MJ, (eds). Woodhead Publishing, p 379–420
King F, Kolar M, Keech PG (2014) Simulations of long-term anaerobic corrosion of carbon steel containers in Canadian deep geological repository. Corros Eng Sci Technol 49:455–459
Knapp V, Pevec D (2018) Promises and limitations of nuclear fission energy in combating climate change. Energy Policy 120:94–99
Kolditz O, Bauer S, Bilke L, Böttcher N, Delfs J, Fischer T, Görke U, Kalbacher T, Kosakowski G, McDermott C (2012) OpenGeoSys: an open-source initiative for numerical simulation of thermo-hydro-mechanical/chemical (THM/C) processes in porous media. Environ Earth Sci 67:589–599
Kulik DA, Wagner T, Dmytrieva SV, Kosakowski G, Hingerl FF, Chudnenko KV, Berner UR (2013) GEM-Selektor geochemical modeling package: revised algorithm and GEMS3K numerical kernel for coupled simulation codes. Comput Geosci 17:1–24
Kulik DA, Hummel W, Lützenkirchen J, Lefèvre G (2015) Preface: SI: Geochemical speciation codes and databases. Appl Geochem 55:1–2
Kursten B, Druyts F (2008) Methodology to make a robust estimation of the carbon steel overpack lifetime with respect to the Belgian Supercontainer design. J Nucl Mater 379:91–96
Kursten B, Macdonald DD, Smart NR, Gaggiano R (2017) Corrosion issues of carbon steel radioactive waste packages exposed to cementitious materials with respect to the Belgian supercontainer concept. Corros Eng Sci Technol 52:11–16
L'Hostis V, Amblard E, Blanc C, Miserque F, Paris C, Bellot-Gurlet L (2011) Passive corrosion of steel in concrete in context of nuclear waste disposal. Corros Eng Sci Technol 46:177–181
Lalan P, Dauzeres A, De Windt L, Bartier D, Sammaljarvi J, Barnichon JD, Techer I, Detilleux V (2016) Impact of a 70 °C temperature on an ordinary Portland cement paste/claystone interface: An in situ experiment. Cem Concr Res 83:164–178
Landais P, Aranyossy J-F (2011) Clays in natural and engineered barriers for radioactive waste confinement. Phys Chem Earth, Parts A/B/C 36:1437
Landrot G, Ajo-Franklin JB, Yang L, Cabrini S, Steefel CI (2012) Measurement of accessible reactive surface area in a sandstone, with application to CO_2 mineralization. Chem Geol 318–319:113–125
Lassin A, Azaroual M, Mercury L (2005) Geochemistry of unsaturated soil systems: Aqueous speciation and solubility of minerals and gases in capillary solutions. Geochim Cosmochim Acta 69:5187–5201
Lassin A, Dymitrowska M, Azaroual M (2011) Hydrogen solubility in pore water of partially saturated argillites: Application to Callovo–Oxfordian clayrock in the context of a nuclear waste geological disposal. Phys Chem Earth, Parts A/B/C 36:1721–1728
Lassin A, Marty NCM, Gailhanou H, Henry B, Trémosa J, Lerouge C, Madé B, Altmann S, Gaucher EC (2016) Equilibrium partial pressure of CO_2 in Callovian–Oxfordian argillite as a function of relative humidity: Experiments and modelling. Geochim Cosmochim Acta 186:91–104
Lerouge C, Vinsot A, Grangeon S, Wille G, Flehoc C, Gailhanou H, Gaucher EC, Madé B, Altmann S, Tournassat C (2013) Controls of Ca/Mg/Fe activity ratios in pore water chemistry models of the Callovian–Oxfordian Clay formation. Procedia Earth Planet Sci 7:475–478
Lerouge C, Gaboreau S, Grangeon S, Claret F, Warmont F, Jenni A, Cloet V, Mäder U (2017) In situ interactions between opalinus clay and low alkali concrete. Phys Chem Earth, Parts A/B/C 99:3–21

Lerouge C, Robinet JC, Debure M, Tournassat C, Bouchet A, Fernández AM, Flehoc C, Guerrot C, Kars M, Lagroix F, Landrein P (2018) A deep alteration and oxidation profile in a shallow clay aquitard: Example of the Tégulines Clay, East Paris Basin, France. Geofluids 2018:20

Leterrier N, Bary B (2011) Fully Coupled Unsaturated Hydraulics and Reactive Transport Model for the Simulation of Concrete Carbonation. J Nucl Res Dev 2:11–18

Li L (2019) Watershed reactive transport. Rev Mineral Geochem 85:381–418

Lichtner PC (1996) Continuum formulation of multicomponent-multiphase reactive transport. *In:* Reactive Transp Porous Media. Vol 34. Lichtner PC, Steefel CI, Oelkers EH, (eds). p 1–81

Linsley G, Fattah A (1994) The interface between nuclear safeguards and radioactive waste disposal: Emerging issues. IAEA Bulletin 36:22–26

Lisjak A, Garitte B, Grasselli G, Müller HR, Vietor T (2015) The excavation of a circular tunnel in a bedded argillaceous rock (Opalinus Clay): Short-term rock mass response and FDEM numerical analysis. Tunnelling and Underground Space Technol 45:227–248

Liu S, Ferrand K, Lemmens K (2015) Transport and surface reaction-controlled SON68 glass dissolution at 30 °C and 70 °C and pH=13.7. Appl Geochem 61:302–311

Lothenbach B (2010) Thermodynamic equilibrium calculations in cementitious systems. Mater Struct 43:1413–1433

Lothenbach B, Wieland E (2006) A thermodynamic approach to the hydration of sulphate-resisting Portland cement. Waste Manage 26:706–719

Lothenbach B, Winnefeld F (2006) Thermodynamic modelling of the hydration of Portland cement. Cem Concr Res 36:209–226

Lothenbach B, Rentsch D, Wieland E (2014) Hydration of a silica fume blended low-alkali shotcrete cement. Phys Chem Earth 70–71:3–16

Lothenbach B, Le Saout G, Ben Haha M, Figi R, Wieland E (2012) Hydration of a low-alkali CEM III/B–SiO_2 cement (LAC). Cem Concr Res 42:410–423

Lothenbach B, Kulik DA, Matschei T, Balonis M, Baquerizo L, Dilnesa B, Miron GD, Myers RJ (2019) Cemdata 18: A chemical thermodynamic database for hydrated Portland cements and alkali-activated materials. Cem Concr Res 115:472–506

Lu C, Samper J, Fritz B, Clement A, Montenegro L (2011) Interactions of corrosion products and bentonite: An extended multicomponent reactive transport model. Phys Chem Earth, Parts A/B/C 36:1661–1668

Luke K, Lachowski E (2008) Internal composition of 20-year-old fly ash and slag-blended ordinary Portland cement Pastes. J Am Ceram Soc 91:4084–4092

Macdonald DD, Urquidi-Macdonald M, Engelhardt GR, Azizi O, Saleh A, Almazooqi A, Rosas-Camacho O (2011) Some important issues in electrochemistry of carbon steel in simulated concrete pore water Part 1: Theoretical issues. Corros Eng Sci Technol 46:98–103

Marschall P, Horseman S, Gimmi T (2005) Characterisation of gas transport properties of the Opalinus Clay, a potential host rock formation for radioactive waste disposal. Oil Gas Sci Technol – Rev IFP 60:121–139

Martin FA, Bataillon C, Schlegel ML (2008) Corrosion of iron and low alloyed steel within a water saturated brick of clay under anaerobic deep geological disposal conditions: An integrated experiment. J Nucl Mater 379:80–90

Martin LHJ, Leemann A, Milodowski AE, Mader UK, Munch B, Giroud N (2016) A natural cement analogue study to understand the long-term behaviour of cements in nuclear waste repositories: Maqarin (Jordan). Appl Geochem 71:20–34

Marty NCM, Tournassat C, Burnol A, Giffaut E, Gaucher EC (2009) Influence of reaction kinetics and mesh refinement on the numerical modelling of concrete/clay interactions. J Hydrol 364:58–72

Marty NCM, Fritz B, Clément A, Michau N (2010) Modelling the long term alteration of the engineered bentonite barrier in an underground radioactive waste repository. Appl Clay Sci 47:82–90

Marty NM, Munier I, Gaucher E, Tournassat C, Gaboreau S, Vong C, Giffaut E, Cochepin B, Claret F (2014) Simulation of Cement/Clay Interactions: Feedback on the Increasing Complexity of Modelling Strategies. Transp Porous Media 104:385–405

Marty NCM, Claret F, Lassin A, Tremosa J, Blanc P, Madé B, Giffaut E, Cochepin B, Tournassat C (2015a) A database of dissolution and precipitation rates for clay-rocks minerals. Appl Geochem 55:108–118

Marty NC, Bildstein O, Blanc P, Claret F, Cochepin B, Gaucher EC, Jacques D, Lartigue JE, Liu S, Mayer KU, Meeussen JC (2015b) Benchmarks for multicomponent reactive transport across a cement/clay interface. Comput Geosci 19:635–653

Matray JM, Savoye S, Cabrera J (2007) Desaturation and structure relationships around drifts excavated in the well-compacted Tournemire's argillite (Aveyron, France). Eng Geol 90:1–16

Mayer KU, Frind EO, Blowes DW (2002) Multicomponent reactive transport modeling in variably saturated porous media using a generalized formulation for kinetically controlled reactions. Water Resour Res 38:13–11-13–21

McGrail BP, Chick LA (1984) Initial resultats for the experimental evaluation of a nuclear waste reposity source term model. Nucl Technol 69:114–118

Meeussen JCL (2003) ORCHESTRA: An object-oriented framework for implementing chemical equilibrium models. Environ Sci Technol 37:1175–1182

Mercado-Depierre S, Angeli F, Frizon F, Gin S (2013) Antagonist effects of calcium on borosilicate glass alteration. J Nucl Mater 441:402–410

Mercado-Depierre S, Fournier M, Gin S, Angeli F (2017) Influence of zeolite precipitation on borosilicate glass alteration under hyperalkaline conditions. J Nucl Mater 491:67–82
Meserve RA (2004) Global warming and nuclear power. Science 303:433
Molins S, Knabner P (2019) Multiscale approaches in reactive transport modeling. Rev Mineral Geochem 85:27–48
Mon A, Samper J, Montenegro L, Naves A, Fernandez J (2017) Long-term non-isothermal reactive transport model of compacted bentonite, concrete and corrosion products in a HLW repository in clay. J Contam Hydrol 197:1–16
Montarnal P, Mugler C, Colin J, Descostes M, Dimier A, Jacquot E (2007) Presentation and use of a reactive transport code in porous media. Phys Chem Earth 32:507–517
Montes-H G, Fritz B, Clement A, Michau N (2005) Modeling of transport and reaction in an engineered barrier for radioactive waste confinement. Appl Clay Sci29:155–171
Mosser-Ruck R, Cathelineau M, Guillaume D, Charpentier D, Rousset D, Barres O, Michau N (2010) Effects of temperature, ph, and iron/clay and liquid/clay ratios on experimental conversion of dioctahedral smectite to berthierine, chlorite, vermiculite, or saponite. Clays Clay Miner 58:280–291
Müller HR, Garitte B, Vogt T, Köhler S, Sakaki T, Weber H, Spillmann T, Hertrich M, Becker JK, Giroud N, Cloet V (2018) Implementation of the full-scale emplacement (FE) experiment at the Mont Terri rock laboratory. Swiss J Geosci 110:287–306
Mürmann M, Kühn M, Pape H, Clauser C (2013) Numerical simulation of pore size dependent anhydrite precipitation in geothermal reservoirs. Energy Proced 40:107–116
Nagra (2002) Project Opalinus Clay. Models, Codes and Data for Safety Assessment. Demonstration of disposal feasibility for spent fuel, vitrified high-level waste and long-lived intermediate-level waste. NAGRA Technical Report 02–06
Necib S, Linard Y, Crusset D, Michau N, Daumas S, Burger E, Romaine A, Schlegel ML (2016) Corrosion at the carbon steel-clay borehole water and gas interfaces at 85 °C under anoxic and transient acidic conditions. Corrosion Science 111:242–258
Ngo VV, Delalande M, Clément A, Michau N, Fritz B (2014) Coupled transport-reaction modeling of the long-term interaction between iron, bentonite and Callovo–Oxfordian claystone in radioactive waste confinement systems. Appl Clay Sci101:430–443
Ngo VV, Clément A, Michau N, Fritz B (2015) Kinetic modeling of interactions between iron, clay and water: Comparison with data from batch experiments. Appl Geochem 53:13–26
Noguera C, Fritz B, Clément A, Baronnet A (2006) Nucleation, growth and ageing scenarios in closed systems I: A unified mathematical framework for precipitation, condensation and crystallization. J Cryst Growth 297:180–186
Noguera C, Fritz B, Clément A (2016) Kinetics of precipitation of non-ideal solid-solutions in a liquid environment. Chem Geol 431:20–35
Noiriel C, Steefel CI, Yang L, Ajo-Franklin J (2012) Upscaling calcium carbonate precipitation rates from pore to continuum scale. Chem Geol 318–319:60–74
Odorowski M, Jegou C, De Windt L, Broudic V, Jouan G, Peuget S, Martin C (2017) Effect of metallic iron on the oxidative dissolution of UO_2 doped with a radioactive alpha emitter in synthetic Callovian-Oxfordian groundwater. Geochim Cosmochim Acta 219:1–21
Ondraf/Niras (2009) The long-term safety strategy for the geological disposal of radioactive waste, SFC1 level 4 report: second full draft', Report no. NIROND-TR 2009–12E, Ondraf/Niras, Brussels, Belgium.
Park DC (2008) Carbonation of concrete in relation to CO_2 permeability and degradation of coatings. Construction and Building Materials 22:2260–2268
Parkhurst DL, Appelo C (1999) User's guide to PHREEQC (Version 2): A computer program for speciation, batch-reaction, one-dimensional tansport, and inverse geochemical calculations.
Peña J, Torres E, Turrero MJ, Escribano A, Martin PL (2008) Kinetic modelling of the attenuation of carbon steel canister corrosion due to diffusive transport through corrosion product layers. Corrosion Science 50:2197–2204
Pfingsten W, Paris B, Soler J, Mäder U (2006) Tracer and reactive transport modelling of the interaction between high-pH fluid and fractured rock: Field and laboratory experiments. Journal of Geochemical Exploration 90:95–113
Poinssot C, Gin S (2012) Long-term Behavior Science: The cornerstone approach for reliably assessing the long-term performance of nuclear waste. J Nucl Mater420:182–192
Poinssot C, Fillet C, Gras JM (2010) 14 - Post-containment performance of geological repository systems: source-term release and radionuclide migration in the near- and far-field environments. *In:* Geological Repository Systems for Safe Disposal of Spent Nuclear Fuels and Radioactive Waste. Ahn J, Apted MJ, (eds). Woodhead Publishing, p 421–493
Poller A, Enssle CP, Mayer G, Croisé J, Wendling J (2011) Repository-scale modeling of the long-term hydraulic perturbation induced by gas and heat generation in a geological repository for high-and intermediate-level radioactive waste: methodology and example of application. Transp Porous Media 90:77–94
Pozo C, Bildstein O, Raynal J, Jullien M, Valcke E (2007) Behaviour of silicon released during alteration of nuclear waste glass in compacted clay. Appl Clay Sci 35:258–267
Ragoussi M-E, Costa D (2019) Fundamentals of the NEA Thermochemical database and its influence over national nuclear programs on the performance assessment of deep geological repositories. J Environ Radioact 196:225–231

Rajmohan N, Frugier P, Gin S (2010) Composition effects on synthetic glass alteration mechanisms: Part 1. Experiments. Chem Geol 279:106–119
Rajyaguru A, L'Hôpital E, Savoye S, Wittebroodt C, Bildstein O, Arnoux P, Detilleux V, Fatnassi I, Gouze P, Lagneau V (2019) Experimental characterization of coupled diffusion reaction mechanisms in low permeability chalk. Chem Geol 503:29–39
Rebiscoul D, Tormos V, Godon N, Mestre JP, Cabie M, Amiard G, Foy E, Frugier P, Gin S (2015) Reactive transport processes occurring during nuclear glass alteration in presence of magnetite. Appl Geochem 58:26–37
Ribet S, Gin S (2004) Role of neoformed phases on the mechanisms controlling the resumption of SON68 glass alteration in alkaline media. J Nucl Mater324:152–164
Roosz C, Vieillard P, Blanc P, Gaboreau S, Gailhanou H, Braithwaite D, Montouillout V, Denoyel R, Henocq P, Made B (2018) Thermodynamic properties of C-S-H, C-A-S-H and M-S-H phases: Results from direct measurements and predictive modelling. Appl Geochem 92:140–156
Saheb M, Berger P, Raimbault L, Neff D, Dillmann P (2012) Investigation of iron long-term corrosion mechanisms in anoxic media using deuterium tracing. J Nucl Mater 423:61–66
Samper J, Yang C, Montenegro L (2003) User's manual of CORE2D Version 4: A code for ground-water flow and reactive solute transport: La Coruña. Universidad de A Coruña, Spain
Samper J, Lu C, Montenegro L (2008) Reactive transport model of interactions of corrosion products and bentonite. Phys Chem Earth, Parts A/B/C 33:S306-S316
Samper J, Naves A, Montenegro L, Mon A (2016) Reactive transport modelling of the long-term interactions of corrosion products and compacted bentonite in a HLW repository in granite: Uncertainties and relevance for performance assessment. Appl Geochem 67:42–51
Samper J, Mon A, Montenegro L, Cuevas J, Turrero MJ, Naves A, Fernandez R, Torres E (2018) Coupled THCM model of a heating and hydration concrete-bentonite column test. Appl Geochem 94:67–81
Savage D, Cloet V (2018) A review of cement–clay modelling, Nagra Working Report NAB 18-24, Nagra, Wettingen, Switzerland.
Savage D, Noy D, Mihara M (2002) Modelling the interaction of bentonite with hyperalkaline fluids. Appl Geochem 17:207–223
Savage D, Walker C, Arthur R, Rochelle C, Oda C, Takase H (2007) Alteration of bentonite by hyperalkaline fluids: A review of the role of secondary minerals. Phys Chem Earth 32:287–297
Savage D, Watson C, Benbow S, Wilson J (2010) Modelling iron-bentonite interactions. Appl Clay Sci 47:91–98
Savija B, Lukovic M (2016) Carbonation of cement paste: Understanding, challenges, and opportunities. Construction and Building Materials 117:285–301
Schlegel ML, Bataillon C, Blanc C, Prêt D, Foy E (2010) Anodic activation of iron corrosion in clay media under water-saturated conditions at 90 °C: Characterization of the corrosion interface. Environ Sci Technol 44:1503–1508
Schlegel ML, Bataillon C, Brucker F, Blanc C, Prêt D, Foy E, Chorro M (2014) Corrosion of metal iron in contact with anoxic clay at 90°C: Characterization of the corrosion products after two years of interaction. Appl Geochem 51:1–14
Schlegel ML, Necib S, Daumas S, Blanc C, Foy E, Trcera N, Romaine A (2016) Microstructural characterization of carbon steel corrosion in clay borehole water under anoxic and transient acidic conditions. Corros Sci 109:126–144
Schlegel ML, Necib S, Daumas S, Labat M, Blanc C, Foy E, Linard Y (2018) Corrosion at the carbon steel-clay borehole water interface under anoxic alkaline and fluctuating temperature conditions. Corros Sci 136:70–90
Sedighi M, Thomas HR, Al Masum S, Vardon PJ, Nicholson D, Chen Q (2015) Geochemical modelling of hydrogen gas migration in an unsaturated bentonite buffer. Geol Soc , London, Spec Publ 415:189
Seigneur N, Lagneau V, Corvisier J, Dauzères A (2018) Recoupling flow and chemistry in variably saturated reactive transport modelling - An algorithm to accurately couple the feedback of chemistry on water consumption, variable porosity and flow. Adv Water Resour 122:355–366
Seigneur N, Mayer KU, Steefel CI (2019) Reactive transport in evolving porous media. Rev Mineral Geochem 85:197–238
Sellin P, Leupin OX (2013) The use of clay as an engineered barrier in radioactive-waste management - a review. Clays Clay Miner 61:477–498
Sena C, Salas J, Arcos D (2010) Aspects of geochemical evolution of the SKB near field in the frame of SR-Site. SKB report TR-10–59, Swedish Nuclear Fuel and Waste Management Company, Stockholm, Sweden
Senger R, Ewing J, Zhang K, Avis J, Marschall P, Gaus I (2011) Modeling approaches for investigating gas migration from a deep low/intermediate level waste repository (Switzerland). Transp Porous Media 90:113–133
Sercombe J, Gwinner B, Tiffreau C, Simondi-Teisseire B, Adenot F (2006) Modelling of bituminized radioactive waste leaching. Part I: Constitutive equations. J Nucl Mater 349:96–106
Shao HB, Kosakowski G, Berner U, Kulik DA, Mader U, Kolditz O (2013) Reactive transport modeling of the clogging process at Maqarin natural analogue site. Phys Chem Earth 64:21–31
Sherar BWA, Keech PG, Shoesmith DW (2011) Carbon steel corrosion under anaerobic-aerobic cycling conditions in near-neutral pH saline solutions. Part 2: Corrosion mechanism. Corros Sci 53:3643–3650
Sin I, Corvisier J (2019) Multiphase multicomponent reactive transport and flow modeling. Rev Mineral Geochem 85:143–195
SKB (2006) Long-term safety for KBS-3 repositories at Forsmark and Laxemar – a first evaluation Main Report of the SR-Can project, Technical Report TR-06–09, Svensk Kärnbränslehantering AB, Sweden.

Smart NR, Rance AP, Carlson L, Werme LOC (2006) Further studies of the anaerobic corrosion of steel in bentonite. MRS Proceedings 932:32.31
Smart NR, Rance AP, Fennell PAH, Kursten B (2013) The anaerobic corrosion of carbon steel in alkaline media: Phase 2 results. EPJ Web of Conferences 56
Soler JM (2003) Reactive transport modeling of the interaction between a high-pH plume and a fractured marl: the case of Wellenberg. Appl Geochem 18:1555–1571
Soler JM (2016) Two-dimensional reactive transport modeling of the alteration of a fractured limestone by hyperalkaline solutions at Maqarin (Jordan). Appl Geochem 66:162–173
Soler JM, Mader UK (2007) Mineralogical alteration and associated permeability changes induced by a high-pH plume: Modeling of a granite core infiltration experiment. Appl Geochem 22:17–29
Spycher NF, Sonnenthal EL, Apps JA (2003) Fluid flow and reactive transport around potential nuclear waste emplacement tunnels at Yucca Mountain, Nevada. J Contam Hydrol 62–63:653–673
Steefel CI, Vancappellen P (1990) A new kinetic approach to modeling water–rock interaction—the role of nucleation, precursors, and Ostwald ripening. Geochim Cosmochim Acta 54:2657–2677
Steefel CI, Lichtner PC (1998) Multicomponent reactive transport in discrete fractures: II: Infiltration of hyperalkaline groundwater at Maqarin, Jordan, a natural analogue site. J Hydrol 209:200–224
Steefel CI, DePaolo DJ, Lichtner PC (2005) Reactive transport modeling: An essential tool and a new research approach for the Earth sciences. Earth Planet Sci Lett 240:539–558
Steefel CI, Appelo CA, Arora B, Jacques D, Kalbacher T, Kolditz O, Lagneau V, Lichtner PC, Mayer KU, Meeussen JC, Molins S (2014) Reactive transport codes for subsurface environmental simulation. Comput Geosci:1–34
Steefel C, Beckingham L, Landrot G (2015a) Micro-continuum approaches for modeling pore–scale geochemical processes. Rev Mineral Geochem 80:217–246
Steefel CI, Appelo CA, Arora B, Jacques D, Kalbacher T, Kolditz O, Lagneau V, Lichtner PC, Mayer KU, Meeussen JC, Molins S (2015b) Reactive transport codes for subsurface environmental simulation. Comput Geosci 19:445–478
Talandier J, Mayer G, Croisé J (2006) Simulations of the hydrogen migration out of intermediate-level radioactive waste disposal drifts using tough2. TOUGH Symposium, May 15–17, 2006, Lawrence Berkeley National Laboratory, Berkeley, California
Thatcher KE, Bond AE, Norris S (2016) Engineered damage zone sealing during a water injection test at the Tournemire URL. Environ Earth Sci 75:933
Thiery M (2005) Modelling of atmospheric carbonation of cement based materials considering the kinetic effects and modifications of the microstructure and the hydric state. PhD thesis, Ecole des Ponts ParisTech, Paris
Thiery M, Villain G, Dangla P, Platret G (2007) Investigation of the carbonation front shape on cementitious materials: Effects of the chemical kinetics. Cem Concr Res 37:1047–1058
Thiery M, Dangla P, Belin P, Habert G, Roussel N (2013) Carbonation kinetics of a bed of recycled concrete aggregates: A laboratory study on model materials. Cem Concr Res 46:50–65
Thouvenot P, Bildstein O, Munier I, Cochepin B, Poyet S, Bourbon X, Treille E (2013) Modeling of concrete carbonation in deep geological disposal of intermediate level waste. EPJ Web of Conferences 56:05004
Tinseau E, Bartier D, Hassouta L, Devol-Brown I, Stammose D (2006) Mineralogical characterization of the Tournemire argillite after in situ interaction with concretes. Waste Manage 26:789–800
Tournassat C, Steefel CI (2019) Reactive transport modeling of coupled processes in nanoporous media. Rev Mineral Geochem 85:75–109
Treille E, Wendling J, Trenty L, Loth L, Pépin G, Plas F (2012) Probabilistic analysis based on simulations of the long-term gas migration at repository-scale in a geological repository for high and intermediate level radioactive waste disposal in a deep clay formation. Proceedings TOUGH Symposium, Lawrence Berkeley National Laboratory, Berkeley, California, September 17–19, 2012
Trotignon L, Peycelon H, Bourbon X (2006) Comparison of performance of concrete barriers in a clayey geological medium. Phys Chem Earth 31:610–617
Trotignon L, Devallois V, Peycelon H, Tiffreau C, Bourbon X (2007) Predicting the long term durability of concrete engineered barriers in a geological repository for radioactive waste. Phys Chem Earth 32:259–274
Trotignon L, Thouvenot P, Munier I, Cochepin B, Piault E, Treille E, Bourbon X, Mimid S (2011) Numerical simulation of atmpspheric carbonation of concrete components in a deep geological radwaste disposal during operating period. Nucl Technol 174:424–437
Trinchero P, Puigdomenech I, Molinero J, Ebrahimi H, Gylling B, Svensson U, Bosbach D, Deissmann G (2017) Continuum-based DFN-consistent numerical framework for the simulation of oxygen infiltration into fractured crystalline rocks. J Contam Hydrol 200:60–69
Truche L, Berger G, Destrigneville C, Pages A, Guillaume D, Giffaut E, Jacquot E (2009) Experimental reduction of aqueous sulphate by hydrogen under hydrothermal conditions: Implication for the nuclear waste storage. Geochim Cosmochim Acta 73:4824–4835
Tsang C-F, Gelhar L, de Marsily G, Andersson J (1994) Solute transport in heterogeneous media: A discussion of technical issues coupling site characterization and predictive assessment. Adv Water Resour 17:259–264

Ufer K, Stanjek H, Roth G, Dohrmann R, Kleeberg R, Kaufhold S (2008) Quantitative phase analysis of bentonites by the Rietveld method. Clays Clay Miner 56:272–282

Van Damme H, Pellenq RJM, Ulm FJ (2013) Chapter 14.3 - Cement Hydrates. *In:* Developments in Clay Science. Vol Volume 5. Faïza B, Gerhard L, (eds). Elsevier, p 801–817

van der Lee J, De Windt L, Lagneau V, Goblet P (2003) Module-oriented modeling of reactive transport with HYTEC. Comput Geosci 29:265–275

Vinsot A, Linard Y, Lundy M, Necib S, Wechner S (2013) Insights on desaturation processes based on the chemistry of seepage water from boreholes in the Callovo–Oxfordian argillaceous rock. Procedia Earth Planet Sci 7:871–874

Vinsot A, Leveau F, Bouchet A, Arnould A (2014) Oxidation front and oxygen transfer in the fractured zone surrounding the Meuse/Haute-Marne URL drifts in the Callovian–Oxfordian argillaceous rock. Geol Soc London, Spec Publ 400:207–220

Vinsot A, Lundy M, Linard Y (2017) O_2 consumption and CO_2 production at Callovian–Oxfordian rock surfaces. Procedia Earth Planet Sci 17:562–565

von Schenck H, Källström K (2014) Reactive transport modelling of organic complexing agents in cement stabilized low and intermediate level waste. Phys Chem Earth, Parts A/B/C 70–71:114–126

Wagner T, Kulik DA, Hingerl FF, Dmytrieva SV (2012) GEM-SELEKTOR geochemical modeling package: TSolMod library and data interface for multicomponent phase models. Can Mineral 50:1173–1195

Walker CS, Sutou S, Oda C, Mihara M, Honda A (2016) Calcium silicate hydrate (C-S-H) gel solubility data and a discrete solid phase model at 25 °C based on two binary non-ideal solid solutions. Cem Concr Res79:1–30

Wanner H (2007) Solubility data in radioactive waste disposal. Pure Appl Chem 79:875–882

Watson C, Hane K, Savage D, Benbow S, Cuevas J, Fernandez R (2009) Reaction and diffusion of cementitious water in bentonite: Results of 'blind' modelling. Appl Clay Sci 45:54–69

Watson C, Wilson J, Savage D, Benbow S, Norris S (2016) Modelling reactions between alkaline fluids and fractured rock: The Maqarin natural analogue. Appl Clay Sci 121:46–56

Watson C, Wilson J, Savage D, Norris S (2018) Coupled reactive transport modelling of the international Long-Term Cement Studies project experiment and implications for radioactive waste disposal. Appl Geochem 97:134–146

Wersin P (2003) Geochemical modelling of bentonite porewater in high-level waste repositories. J Contam Hydrol 61:405–422

Wersin P, Birgersson M (2014) Reactive transport modelling of iron-bentonite interaction within the KBS-3H disposal concept: the Olkiluoto site as a case study. Geol Soc London, Spec Publ 400:SP400.424

Wersin P, Birgersson M, Karnland O, Snellman M (2008) Impact of corrosion-derived iron on the bentonite buffer within the KBS-3H disposal concept. SKB report TR-08–34

Wilson JC, Benbow S, Sasamoto H, Savage D, Watson C (2015) Thermodynamic and fully coupled reactive transport models of a steel-bentonite interface. Appl Geochem 61:10–28

Wilson JC, Benbow S, Metcalfe R (2018) Reactive transport modelling of a cement backfill for radioactive waste disposal. Cem Concr Res 111:81–93

Wolery TJ (1983) EQ3NR a computer program for geochemical aqueous speciation-solubility calculations: user's guide and documentation. Lawrence Livermore Nat. Lab. UCRL-53414-report, Livermore, CA, USA.

Xu T, Sonnenthal E, Spycher N, Pruess K (2004) TOUGHREACT user's guide: a simulation program for non-isothermal multiphase reactive geochemical transport in variable saturated geologic media. Lawrence Berkeley National Laboratory Report LBNL-55460, Berkeley, USA

Xu T, Senger R, Finsterle S (2008) Corrosion-induced gas generation in a nuclear waste repository: Reactive geochemistry and multiphase flow effects. Appl Geochem 23:3423–3433

Yang C, Samper J, Montenegro L (2008) A coupled non-isothermal reactive transport model for long-term geochemical evolution of a HLW repository in clay. Environ Geol 53:1627–1638

Yeh GT, Tripathi VS (1989) A critical evaluation of recent developments in hydrogeochemical transport models of reactive multichemical components. Water Resour Res 25:93–108

Zeelmaekers E, Honty M, Derkowski A, Srodon J, De Craen M, Vandenberghe N, Adriaens R, Ufer K, Wouters L (2015) Qualitative and quantitative mineralogical composition of the Rupelian Boom Clay in Belgium. Clay Miner 50:249–272

Zhang Z, Thiery M, Baroghel-Bouny V (2015) Numerical modelling of moisture transfers with hysteresis within cementitious materials: Verification and investigation of the effects of repeated wetting–drying boundary conditions. Cem Concr Res 68:10–23

Zheng L, Samper J, Montenegro L, Mayor JC (2008) Multiphase flow and multicomponent reactive transport model of the ventilation experiment in Opalinus clay. Phys Chem Earth, Parts A/B/C 33, Suppl 1:S186-S195

Zheng L, Rutqvist J, Birkholzer JT, Liu H-H (2015) On the impact of temperatures up to 200 °C in clay repositories with bentonite engineer barrier systems: A study with coupled thermal, hydrological, chemical, and mechanical modeling. Eng Geol 197:278–295